
Functional Properties of the Focal-Entropy

Jaimin Shah
University of Minnesota,
USA

Martina Cardone
University of Minnesota,
USA

Alex Dytso
Qualcomm Flarion Technology, Inc.,
USA

Abstract

The focal-loss has become a widely used alternative to cross-entropy in class-imbalanced classification problems, particularly in computer vision. Despite its empirical success, a systematic information-theoretic study of the focal-loss remains incomplete. In this work, we adopt a distributional viewpoint and study the *focal-entropy*, a focal-loss analogue of the cross-entropy. Our analysis establishes conditions for finiteness, convexity, and continuity of the *focal-entropy*, and provides various asymptotic characterizations. We prove the existence and uniqueness of the focal-entropy minimizer, describe its structure, and show that it can depart significantly from the data distribution. In particular, we rigorously show that the focal-loss amplifies mid-range probabilities, suppresses high-probability outcomes, and, under extreme class imbalance, induces an *over-suppression regime* in which very small probabilities are further diminished. These results, which are also experimentally validated, offer a theoretical foundation for understanding the focal-loss and clarify the trade-offs that it introduces when applied to imbalanced learning tasks.

1 Introduction

In learning-based prediction and decision-making, loss functions shape the decision rule and strongly influence performance. Selecting an appropriate loss is therefore critical. A widely used choice is the *log-loss*,

defined for $p \in (0, 1]$ as

$$\mathsf{L}(p) = \log\left(\frac{1}{p}\right). \quad (1)$$

When predicting with a distribution Q_X , the actual outcome $x \in \mathcal{X}$ occurs with probability $P_X(x)$. The log-loss in this case is $\mathsf{L}(Q_X(x)) = \log\frac{1}{Q_X(x)}$. Averaging with respect to the true distribution P_X yields the expected log-loss, which equals the *cross-entropy* of Q_X relative to P_X . Formally, this cross-entropy over \mathcal{X} is defined as

$$H(P_X, Q_X) = \begin{cases} \mathbb{E}_{X \sim P_X} [\mathsf{L}(Q_X(X))] & P_X \ll Q_X, \\ \infty & \text{otherwise.} \end{cases} \quad (2)$$

Despite its ubiquity, the log-loss often performs poorly under class imbalance – common in tasks such as object detection (Lin et al., 2017), fraud detection (He and Garcia, 2009), natural language processing (Li et al., 2020a), and various medical applications (Al Rahhal et al., 2019; Vongkulbhisal et al., 2019; Shu et al., 2019). To address this, (Lin et al., 2017) proposed the *focal-loss*, now widely adopted, especially in computer vision. Its success arises from a simple modification of the log-loss: a modulating pre-factor is introduced that downweights well-classified (“easy”) examples and emphasizes misclassified (“hard”) ones, often yielding substantial accuracy gains.

Definition 1 (Focal-loss). *Given a focus parameter $\gamma \geq 0$ and a prediction score $p \in (0, 1]$, the focal-loss is defined as*

$$\mathsf{L}_\gamma(p) = \underbrace{(1-p)^\gamma}_{\text{focal term}} \underbrace{\log\left(\frac{1}{p}\right)}_{\text{log-loss}}. \quad (3)$$

Although the focal-loss is empirically effective, a *comprehensive* information-theoretic treatment is still lacking. The cross-entropy has a clear foundation in information theory—minimizing it is equivalent to minimizing the Kullback–Leibler (KL) divergence between model and data—thus providing a principled

optimization landscape. In contrast, the focal-loss alters this landscape in ways not yet fully understood. Characterizing the geometry of the resulting objective and its minimizer(s) is therefore essential.

We adopt a distributional viewpoint and introduce the *focal-entropy*, a focal-loss analogue of the cross-entropy that compares two distributions P_X and Q_X .

Definition 2 (Focal-Entropy). *Given a focus parameter $\gamma \geq 0$, the focal-entropy of Q_X relative to P_X over \mathcal{X} is defined as*

$$H_\gamma(P_X, Q_X) = \begin{cases} \mathbb{E}_{X \sim P_X} [\mathbb{L}_\gamma(Q_X(X))] & P_X \ll Q_X, \\ \infty & \text{otherwise.} \end{cases} \quad (4)$$

For $\gamma = 0$, the focal-entropy in (4) reduces to the cross-entropy in (2). A key defining property of the cross-entropy is that the minimizer over the second parameter Q_X (in the space of all probability mass functions on \mathcal{X}) is equal to P_X , that is,

$$\min_{Q_X} H(P_X, Q_X) = H(P_X, P_X) = H(P_X), \quad (5)$$

where the last expression is the Shannon entropy. As we show in this paper, this property, however, is no longer true for the focal-entropy and, in general, the optimizer is not equal to P_X . In this sense, the focal-loss may not appear to be a proper loss (Brehmer and Gneiting, 2020; Buja et al., 2005). However, recent work (Bao and Charoenphakdee, 2025) has shown that the focal-loss is a variant of proper scoring rules. The structure and basic properties (e.g., existence) of the minimizer, i.e.,

$$P_\gamma^* = \arg \min_{Q_X} H_\gamma(P_X, Q_X) \quad (6)$$

are indeed not fully understood. This paper aims to address this gap by providing a full characterization of P_γ^* and studying many of its properties.

1.1 Notation

The set of all probability mass functions over a (possibly countably infinite) set \mathcal{X} is denoted by $\mathcal{P}(\mathcal{X})$. For $P_X \in \mathcal{P}(\mathcal{X})$, its support is

$$\mathcal{S} = \{x \in \mathcal{X} : P_X(x) > 0\}. \quad (7)$$

We write $P_X \ll Q_X$ to denote absolute continuity of P_X with respect to Q_X . For P_X , we let $p_{\min} = \min_{x \in \mathcal{S}} P_X(x)$ and $p_{\max} = \max_{x \in \mathcal{S}} P_X(x)$. All logarithms are natural. The Lambert function’s principal and negative branches are denoted by $W_0(\cdot)$ and $W_{-1}(\cdot)$, respectively (Corless et al., 1996).

1.2 Literature Review

In (Charoenphakdee et al., 2021), the authors implicitly characterized the minimizer of the focal-entropy for the finite alphabet case. They showed that the minimizing class-posterior under the focal-loss is order preserving (i.e., it maintains the same ordering as the true posterior), leading to the conclusion that the focal-loss is *classification-calibrated*. Building on this, (Mukhoti et al., 2020) demonstrated that the focal-loss not only improves accuracy on challenging datasets but also yields models that are better calibrated than those trained with the cross-entropy. Their analysis provided both theoretical justification—framing the focal-loss as a regularized KL divergence that implicitly maximizes entropy—and empirical evidence across vision and NLP tasks, including robustness under distributional shift. In this work, we give a theoretical basis for one of their key empirical findings: that focal-loss predictions exhibit higher entropy than those from log-loss. Several extensions of the focal-loss have been proposed, from modifying the focal term (Li et al., 2022, 2020b) to making the focus parameter adaptive (Ghosh et al., 2022), and even showing that focal- and log-loss arise as special cases of a broader power-series formulation (Leng et al., 2022). Related directions include class-balanced reweighting (Cui et al., 2019), margin-based methods for long-tailed learning (Cao et al., 2019), and balanced softmax corrections (Ren et al., 2020), each tackling class imbalance from complementary angles. On calibration, recent work such as dual focal-loss (Zhang et al., 2023) and entropy-based generalizations like tilted cross-entropy (Lin et al., 2021) or α -entmax losses (Peters et al., 2019) further highlight the central role of entropy-modulated objectives. Collectively, these advances situate the focal-loss within a broader family of class imbalance- and calibration-aware losses that balance sharpness, entropy, and robustness across regimes.

1.3 Paper Outline and Contributions

Section 2 examines analytical properties of the focal-loss and related functions, focusing on objects such as the inverse of its derivative, which is central to characterizing the focal-entropy minimizer.

Section 3 develops basic functional properties of the focal-entropy. Proposition 4 shows that $\gamma \mapsto H_\gamma(P_X, Q_X)$ is non-increasing and convex. Proposition 5 characterizes its asymptotic behavior for large γ , for both finite and countably infinite supports. Proposition 6 states that the focal-entropy is finite if and only if the cross-entropy is finite. Proposition 7 establishes weak lower semicontinuity and convexity of

$Q \mapsto H_\gamma(P_X, Q)$. Finally, Theorem 1 proves the existence, uniqueness, and structure of the focal-entropy minimizer P_γ^* in (6). For the special case of two-point support, we further derive explicit bounds on P_γ^* , as stated in Proposition 9.

Section 4 focuses on the properties of the minimizer P_γ^* , which shed light on the ability of the focal-loss to address class imbalance. Proposition 10 shows that P_γ^* converges to the uniform distribution as $\gamma \rightarrow \infty$ and provides rates of convergence. To analyze how the focal-entropy transforms P_X into P_γ^* , we study the sequence $p_{(i)} - p_{(i)}^*$, where $p_{(i)}$ denotes the i -th largest entry of P_X and $p_{(i)}^*$ is the i -th largest entry of P_γ^* . Theorem 2 establishes that this sequence has at least one and at most two sign changes. This result enables a rigorous discussion of class imbalance, including the characterization of *exact thresholds* for when small-to-moderate probabilities are amplified (i.e., imbalance is reduced). Furthermore, we show that under extreme class imbalance, i.e., when certain probabilities are very small, the focal-loss does not amplify these probabilities, but instead further suppresses them. We name this *over-suppression regime*. This finding is particularly important for practitioners, as it highlights the need to carefully select γ to avoid such regimes.

To better understand the over-suppression regime, we study trade-offs between the support size, γ , and the values of the data distribution P_X . Proposition 11 shows that for every $\gamma > 0$ and support size $|\mathcal{S}| = 2$, the over-suppression regime is not present. We also conjecture that this holds for $|\mathcal{S}| = 3$ and provide theoretical and numerical evidence supporting this conjecture. Proposition 13 and Proposition 14 establish sufficient conditions under which the over-suppression regime does not exist for arbitrary values of $|\mathcal{S}|$. Finally, Proposition 16 shows that whenever the over-suppression regime does not exist, the data distribution P_X majorizes the minimizer P_γ^* . Taken together, these results characterize how the focal-entropy reshapes the data distribution. Complementing this distributional viewpoint, Proposition 17 provides an information-theoretic interpretation by expressing the focal-entropy in terms of relative entropy.

Section 5 validates our results on both *synthetic* and *real* data (MNIST). Finally, Section 6 concludes the paper. Most proofs are in the appendix and the code for our experiments is available at <https://tinyurl.com/3kjmua9>.

2 Focal-Loss: Analytical Properties

We derive several analytical properties of the focal-loss and related functions that will be useful for the

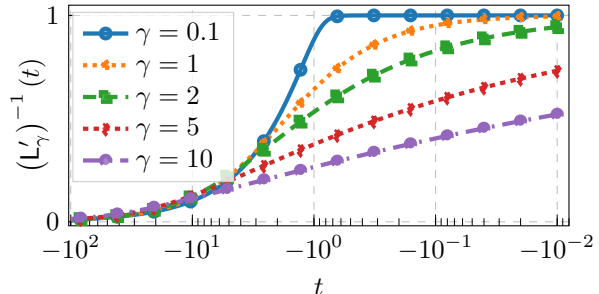


Figure 1: Inverse of L'_γ in (8).

derivation of the results in the subsequent sections of the paper.

In the next proposition (proof in Appendix A.1), we investigate the monotonicity and convexity of the focal-loss function in (3).

Proposition 1. *For $p \in (0, 1)$ and $\gamma \geq 0$, we have the following properties:*

1. $\gamma \mapsto L_\gamma(p)$ is strictly decreasing;
2. $p \mapsto L_\gamma(p)$ is strictly decreasing with the derivative given by

$$L'_\gamma(p) = -(1-p)^{\gamma-1} \left(\gamma \log \frac{1}{p} + \frac{1-p}{p} \right) < 0; \quad (8)$$

3. $p \mapsto L_\gamma(p)$ is strictly convex with the second derivative given by

$$L''_\gamma(p) = \frac{(1-p)^{\gamma-2}}{p^2} [\gamma(1-\gamma)p^2 \log p + 2\gamma p(1-p) + (1-p)^2] > 0. \quad (9)$$

As it will be shown later, the inverse of L'_γ will play an important role in solving the first-order optimality conditions for the focal-entropy minimizer. Some of its important properties are summarized next (proof in Appendix A.2) and also illustrated in Figure 1.

Proposition 2. *For $p \in (0, 1)$, the mapping $p \mapsto L'_\gamma(p)$ has a well-defined inverse $(L'_\gamma)^{-1} : (-\infty, 0) \rightarrow (0, 1)$, which satisfies the following properties:*

1. $(L'_\gamma)^{-1}(-\infty) = 0$ and $(L'_\gamma)^{-1}(0^-) = 1$;
2. $t \mapsto (L'_\gamma)^{-1}(t)$ is strictly increasing;
3. $(L'_\gamma)^{-1}(t) \geq 0$.

The strict monotonicity of $(L'_\gamma)^{-1}$ ensures that the mapping $t \mapsto (L'_\gamma)^{-1}(t)$ is injective (see Figure 1). For $\gamma = 0$ and $\gamma = 1$, we have a closed-form expression for the inverse of (8), which is given by

$$(L'_\gamma)^{-1}(t) = \begin{cases} \frac{1}{W_0(e^{1-t})} & \gamma = 1, \\ -\frac{1}{t} & \gamma = 0. \end{cases} \quad (10)$$

One final function that we will require is

$$\phi_\gamma(p) = -pL'_\gamma(p), \quad p \in (0, 1). \quad (11)$$

The function ϕ_γ will play an important role in Section 4, when we study properties of the minimizer of the focal-entropy. Analyzing its unimodality and bounds helps explain how the focal-loss redistributes probability masses of the data distribution, particularly in imbalanced settings. The next proposition (proof in Appendix A.3) analyzes properties of ϕ_γ in (11).

Proposition 3. *For all $\gamma \geq 0$, the mapping $p \mapsto \phi_\gamma(p)$ satisfies the following properties:*

1. $\phi_\gamma(0^+) = 1$ and $\phi_\gamma(1) = 0$;
2. $p \mapsto \phi_\gamma(p)$ is unimodal. More specifically, the mapping $p \mapsto \phi_\gamma(p)$ is strictly decreasing if $\gamma > \kappa(p)$ and strictly increasing if $\gamma < \kappa(p)$ where

$$\kappa(p) = \frac{1}{p} - \frac{2(1-p)}{p \log\left(\frac{1}{p}\right)}, \quad p \in (0, 1). \quad (12)$$

In addition,

- For $p \in (0, 1)$, $p \mapsto \kappa(p)$ is strictly decreasing;
 - $\kappa(p) \leq 0$ for all $p \in [w, 1)$, where $w = -\frac{1}{2}W_0\left(-\frac{2}{e^2}\right) \approx 0.2032$;
3. $\max_{p \in (0, 1)} \phi_\gamma(p) \leq 1 + \gamma$;
 4. Let $p_\gamma^+ = \arg \max_{p \in (0, 1)} \phi_\gamma(p)$, then

$$p_\gamma^+ \leq \min \left\{ w, \frac{1}{(1 + \sqrt{1 + \gamma})^2} \right\}; \quad (13)$$

5. For $u \in (0, 1/3]$, it holds that $\phi_\gamma(u) \geq \phi_\gamma\left(\frac{1-u}{2}\right)$.

3 Focal-Entropy: Functional Properties

In this section, we develop functional properties of the focal-entropy, proving its convexity, finiteness, and the existence and uniqueness of its minimizer.

3.1 Focal-Entropy vs. γ

We here derive a few properties that highlight how the focal-entropy in (4) varies as a function of γ . The first property is directly derived from the inspection of (4) (see also Appendix B.1, where some additional properties of the mapping $\gamma \mapsto H_\gamma(P_X, Q_X)$ are provided).

Proposition 4. *Fix some $P_X, Q_X \in \mathcal{P}(\mathcal{X})$ such that $P_X \ll Q_X$. For $\gamma \geq 0$, the mapping $\gamma \mapsto H_\gamma(P_X, Q_X)$ is non-increasing and convex. Thus, we have that*

$$0 \leq H_\gamma(P_X, Q_X) \leq H_0(P_X, Q_X) = H(P_X, Q_X). \quad (14)$$

The next proposition (proof in Appendix B.2) presents a limit for the focal-entropy when the focus parameter γ tends to infinity.

Proposition 5. *Fix some $P_X, Q_X \in \mathcal{P}(\mathcal{X})$ such that $P_X \ll Q_X$ and $H(P_X, Q_X) < \infty$. Then, it holds that*

$$\lim_{\gamma \rightarrow \infty} H_\gamma^{\frac{1}{\gamma}}(P_X, Q_X) = \begin{cases} \max_{x \in \mathcal{S}} \bar{Q}_X(x) & |\mathcal{S}| < \infty, \\ 1 & |\mathcal{S}| = \infty, \end{cases} \quad (15)$$

where $\bar{Q}_X(x) = 1 - Q_X(x)$ and \mathcal{S} is defined in (7).

We highlight that, when the support size $|\mathcal{S}|$ is finite, minimizing the right-hand side of (15) over Q_X yields the uniform distribution over \mathcal{S} . A more precise statement of uniformity as $\gamma \rightarrow \infty$ will be given in Proposition 10.

3.2 Basic Functional Properties

We derive some basic functional properties of the focal-entropy in (4). We start with the next proposition (proof in Appendix B.3), which gives a sufficient and necessary condition for the focal-entropy to be finite.

Proposition 6. *Fix some $\gamma \geq 0$. Then, $H_\gamma(P_X, Q_X) < \infty$ if and only if $H(P_X, Q_X) < \infty$.*

For the remainder of the paper, we consider only distributions with *finite* focal-entropy; see (Cover and Thomas, 2006) for an example of infinite entropy. The next proposition (proof in Appendix B.4) presents additional functional properties of the focal-entropy.

Proposition 7. *For any $\gamma \geq 0$ and fixed P_X , it holds that the mapping $Q \mapsto H_\gamma(P_X, Q)$:*

1. is weakly lower semicontinuous¹; and
2. is convex. Moreover, it is strictly convex over the probability space defined on \mathcal{S} in (7).

Remark 1. Proposition 7 shows that the focal-entropy is weakly lower semicontinuous. We note that, in general, the focal-entropy is not weakly continuous. To see this, let $\mathcal{X} = \mathbb{N}$ and consider the distribution

$$P_X(k) = 2^{-k}, \quad k = 1, 2, \dots \quad (16)$$

¹A functional $F : \mathcal{P}(\mathcal{X}) \rightarrow (-\infty, \infty]$ is said to be *weakly lower semicontinuous* if for every sequence $(Q_n)_{n \geq 1}$ such that $Q_n \rightarrow Q$ (weak convergence), we have that $F(Q) \leq \liminf_{n \rightarrow \infty} F(Q_n)$.

Now, for each n , define

$$Q_n(k) = \begin{cases} P_X(k) & k < n, \\ \sum_{j=n}^{\infty} P_X(j) & k = n, \\ 0 & k > n. \end{cases} \quad (17)$$

Then, for every fixed k , $Q_n(k) \rightarrow P_X(k)$ as $n \rightarrow \infty$, so Q_n converges weakly to P_X . However, the fact that $Q_n(k) = 0$ for all $k > n$ with $P_X(k) > 0$, leads to $H_\gamma(P_X, Q_n) = \infty$, whereas $H_\gamma(P_X, P_X) < \infty$. This example shows that H_γ is not weakly continuous.

In (Mukhoti et al., 2020), the authors provided an inequality between the focal-entropy and the cross-entropy, which allows certain learning conclusions to be made. In Proposition 18, we will provide a novel relationship that bounds the difference between their infimum values.

3.3 Optimization of the Focal-Entropy

The minimum of the cross-entropy in (2) (see (5)) follows from the non-negativity of the relative entropy, or equivalently Gibbs' inequality. We now show a similar result for the focal-entropy.

Theorem 1. *Fix some $P_X \in \mathcal{P}(\mathcal{X})$ with support \mathcal{S} as in (7) and $\gamma \geq 0$. Then, there exists a unique $0 < \alpha_\gamma^* < \infty$ such that*

$$P_\gamma^*(x) = \begin{cases} (\mathbb{L}'_\gamma)^{-1} \left(-\frac{\alpha_\gamma^*}{P_X(x)} \right) & x \in \mathcal{S}, \\ 0 & x \notin \mathcal{S}, \end{cases} \quad (18)$$

is a valid distribution. Moreover, for all $Q_X \in \mathcal{P}(\mathcal{X})$, it holds that

$$H_\gamma(P_X, Q_X) \geq H_\gamma(P_X, P_\gamma^*) + \alpha_\gamma^* \left(1 - \sum_{x \in \mathcal{S}} Q_X(x) \right) \quad (19)$$

$$\geq H_\gamma(P_X, P_\gamma^*), \quad (20)$$

and $P_\gamma^* = \arg \min_{Q_X} H_\gamma(P_X, Q_X)$ is the unique minimizer for the focal-entropy.

Proof. For P_γ^* in (18) to be a valid distribution, the constant α_γ^* must be a positive root of the equation $F(\alpha_\gamma^*) = 1$, where

$$F(\alpha) = \sum_{x \in \mathcal{S}} (\mathbb{L}'_\gamma)^{-1} \left(-\frac{\alpha}{P_X(x)} \right), \quad \alpha > 0. \quad (21)$$

From Proposition 2, each summand in (21) is continuous and strictly decreasing in $\alpha > 0$ having values on $(0, 1)$. Thus, $\alpha \mapsto F(\alpha)$ is continuous and strictly decreasing with $F(0^+) = |\mathcal{S}|$ and $F(+\infty) = 0$ (see Proposition 2). Then, by the intermediate value theorem, there is a unique positive root α_γ^* , yielding a valid P_γ^* .

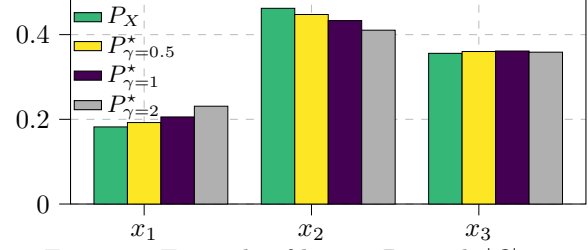


Figure 2: Example of how a P_X with $|\mathcal{S}| = 3$ is transformed into P_γ^* in (18) for different values of γ .

To show the second part of the theorem, recall from Proposition 1 that $p \mapsto \mathbb{L}_\gamma(p)$ is strictly convex and so it can be lower bounded by a tangent line as follows,

$$\mathbb{L}_\gamma(Q(X)) \quad (22)$$

$$\geq \mathbb{L}_\gamma(P_\gamma^*(X)) + \mathbb{L}'_\gamma(P_\gamma^*(X)) (Q(X) - P_\gamma^*(X)) \quad (23)$$

$$= \mathbb{L}_\gamma(P_\gamma^*(X)) - \frac{\alpha_\gamma^*}{P_X(X)} (Q(X) - P_\gamma^*(X)). \quad (24)$$

Consequently, for any choice of Q , we arrive at

$$H_\gamma(P_X, Q) \quad (25)$$

$$= \mathbb{E}[\mathbb{L}_\gamma(Q(X))] \quad (26)$$

$$\geq \mathbb{E}[\mathbb{L}_\gamma(P_\gamma^*(X))] - \mathbb{E} \left[\frac{\alpha_\gamma^*}{P_X(X)} (Q(X) - P_\gamma^*(X)) \right] \quad (27)$$

$$= \mathbb{E}[\mathbb{L}_\gamma(P_\gamma^*(X))] - \alpha_\gamma^* \left(\sum_{x \in \mathcal{S}} Q(x) - 1 \right) \quad (28)$$

$$\geq \mathbb{E}[\mathbb{L}_\gamma(P_\gamma^*(X))] \quad (29)$$

$$= H_\gamma(P_X, P_\gamma^*), \quad (30)$$

where all the expectations are taken with respect to $X \sim P_X$. The fact that P_γ^* in (18) is the unique minimizer for the focal-entropy is due to the convexity result in Proposition 7. \square

Figure 2 illustrates how a distribution P_X with $|\mathcal{S}| = 3$ is transformed into P_γ^* in (18) for different values of γ . The smallest probability (at $x = x_1$) is amplified, while the largest (at $x = x_2$) is reduced. Intuitively, the transformation shifts the mass from high- to low-probability outcomes, mitigating imbalance. Section 4 gives a complete characterization of which probabilities are amplified or suppressed.

Some immediate consequences of Theorem 1 (with Proposition 2) are provided in the next corollary (proof in Appendix B.5).

Corollary 1. *The distribution P_γ^* in Theorem 1 satisfies the following properties:*

1. $P_\gamma^* \ll P_X$;
2. For any $x_1, x_2 \in \mathcal{S}$

$$P_X(x_1) \geq P_X(x_2) \implies P_\gamma^*(x_1) \geq P_\gamma^*(x_2); \quad (31)$$

3. $P_\gamma^* = P_X$ if and only if $\gamma = 0$ or P_X is a uniform distribution.

Remark 2. It is useful to think of the mapping $P_X \mapsto P_\gamma^*$ as an operator. The inverse of this operator is well-defined and has a closed-form expression given by

$$P_X(x) = \frac{\beta}{L'_\gamma(P_\gamma^*(x))}, \quad x \in \mathcal{S}, \quad (32)$$

$$\beta = \left(\sum_{v \in \mathcal{S}} \frac{1}{L'_\gamma(P_\gamma^*(v))} \right)^{-1}. \quad (33)$$

In some cases, this inverse operator is easier to handle due to its closed form. This view relates to (Charoenphakdee et al., 2021, Theorem 11), which derived (32) for finite alphabets via Lagrangian duality. In contrast, Theorem 1 extends the result to countably infinite alphabets and gives a more geometric proof based on the inverse of the focal-loss derivative. Our setting is also more natural in practice: since the optimizer P_γ^* is usually unknown, one typically works with the forward mapping $P_X \mapsto P_\gamma^*$.

The minimizer in (18) depends on α_γ^* and hence, finding bounds on α_γ^* helps to reduce the search space. The next proposition (proof in Appendix B.6) provides bounds on α_γ^* , which will be leveraged for theoretical derivations in the remainder of the paper.

Proposition 8. *For all $\gamma \geq 0$, it holds that*

$$\alpha_\gamma^* \leq \max_{t \in (0,1)} \phi_\gamma(t) \leq 1 + \gamma. \quad (34)$$

Moreover, suppose that $|\mathcal{S}| = N < \infty$. Then:

- For all $\gamma \geq 0$, it holds that

$$p_{\min} c_{N,\gamma} \leq \alpha_\gamma^* \leq p_{\max} c_{N,\gamma}, \quad (35)$$

where $c_{N,\gamma} = -L'_\gamma(1/N) > 0$.

- For all $\gamma > \kappa(p_{\min})$, with $\kappa(\cdot)$ being defined in (12), it holds that

$$\phi_\gamma(p_{\max}) \leq \alpha_\gamma^* \leq \phi_\gamma(p_{\min}). \quad (36)$$

- For all $\gamma < \kappa(p_{\max})$, with $\kappa(\cdot)$ being defined in (12), it holds that

$$\phi_\gamma(p_{\min}) < \alpha_\gamma^* < \phi_\gamma(p_{\max}). \quad (37)$$

Remark 3. The lower and upper bounds in (35), (36), and (37) match when P_X is a uniform distribution.

Remark 4. It is well known that the minimizer of the cross-entropy is *idempotent*: if the minimization procedure is initialized at a distribution P_0^* , the optimizer coincides with the initialization and no further change occurs. In contrast, the minimizer of the focal-entropy

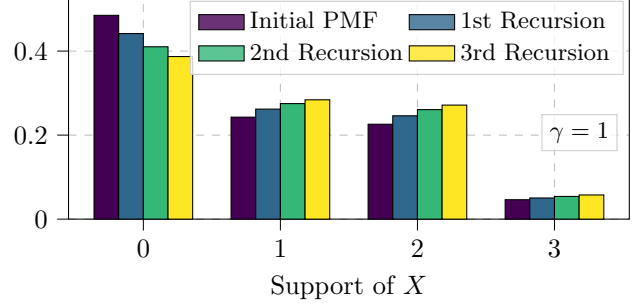


Figure 3: Initial probability mass function:
 $P_X = [0.485 \quad 0.243 \quad 0.226 \quad 0.046]$.

does *not* exhibit this property. As illustrated in Figure 3, the optimizer P_γ^* in (18) is, in general, *not idempotent*. The results shown in Figure 3 were obtained as follows. Starting from the initial probability mass function

$$P_X = [0.485 \quad 0.243 \quad 0.226 \quad 0.046], \quad (38)$$

we numerically determined (using the bounds in Proposition 8) the value of α_γ^* satisfying the normalization condition $F(\alpha_\gamma^*) = 1$, where $F(\cdot)$ is defined in (21). Using this value, we computed the corresponding optimizer P_γ^* via (18) (Recursion 1 in Figure 3), which differs from the initial distribution P_X . Repeating this procedure by reapplying the optimization to the newly obtained distribution (Recursions 2 and 3 in Figure 3) reveals that successive iterates continue to change. Hence, unlike the cross-entropy case, focal-entropy minimization induces a non-trivial transformation of the distribution under repeated application.

An interesting direction for future work is to determine whether this recursive procedure converges to a limiting distribution.

3.4 Two-Point Support

We consider distributions with $|\mathcal{S}| = 2$ for which we aim to study the structure of the optimizer P_γ^* in (18). Without loss of generality, we assume that $\mathcal{X} = \{0, 1\}$. The next proposition (proof in Appendix B.7) provides bounds on P_γ^* .

Proposition 9. *Let $P_X \in \mathcal{P}(\{0, 1\})$ with $P_X(1) = p \in (0, \frac{1}{2}]$, without loss of generality. Then, for any $\gamma > 0$, the unique minimizer in (18) over $\mathcal{P}(\{0, 1\})$ satisfies*

$$\tilde{Q}_\gamma(1) \leq P_\gamma^*(1) \leq \tilde{Q}_{\gamma+1}(1), \quad (39)$$

where

$$\tilde{Q}_\gamma(1) = q_\gamma := \frac{p^{\frac{1}{\gamma}}}{p^{\frac{1}{\gamma}} + (1-p)^{\frac{1}{\gamma}}}, \quad (40)$$

and $\tilde{Q}_\gamma(0) = 1 - \tilde{Q}_\gamma(1)$.

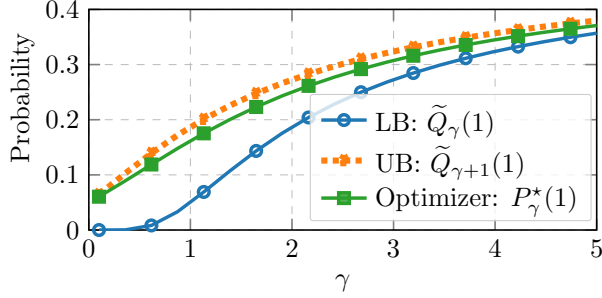
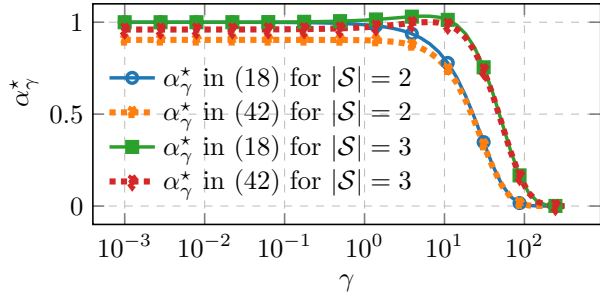


Figure 4: True Probability: 0.05


 Figure 5: Comparison of α_γ^* in (18) with its approximation in (42).

Furthermore, for any $\gamma > 0$, it holds that

$$\tilde{Q}_{\gamma+1}(1) - \tilde{Q}_\gamma(1) \leq \frac{\left| \log \left(\frac{p}{1-p} \right) \right|}{4\gamma^2}. \quad (41)$$

Figure 4 illustrates the performance of the bounds in Proposition 9 in an imbalanced setting, i.e., $p = 0.05$. We observe that the upper bound is tight across the entire range of γ , whereas the lower bound becomes tight for larger values of γ .

4 Properties of the Optimizer

In this section, we explore properties of the optimizer P_γ^* in (18). These are critical since they can shed light on important characteristics of the focal-loss, such as how it helps with class imbalance.

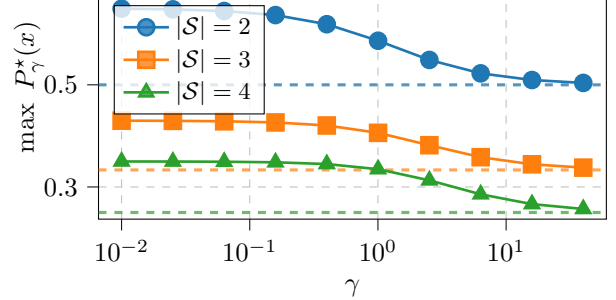
4.1 Large γ Asymptotics of P_γ^*

Our goal here is to understand how P_γ^* in (18) is affected as the value of γ increases. The next proposition (proof in Appendix C.1) answers this question.

Proposition 10. *Suppose that $|\mathcal{S}| < \infty$. Then, as $\gamma \rightarrow \infty$, we have that*

$$\alpha_\gamma^* = -L'_\gamma \left(\frac{1}{|\mathcal{S}|} \right) \text{HM}(P_X) + O \left(\gamma \left(1 - \frac{1}{|\mathcal{S}|} \right)^\gamma \right), \quad (42)$$

$$P_\gamma^*(x) = \frac{1}{|\mathcal{S}|} + O \left(\frac{1}{\gamma} \right), \quad (43)$$


 Figure 6: Convergence of P_γ^* to $1/|\mathcal{S}|$.

where $\text{HM}(P_X) = \frac{|\mathcal{S}|}{\sum_{x \in \mathcal{S}} \frac{1}{P_X(x)}}$ is the harmonic mean of P_X .

Figure 5 compares α_γ^* in (18) with its approximation in (42) for the two following initial distributions

$$P_X = [0.65 \quad 0.35], \text{ for } |\mathcal{S}| = 2, \quad (44)$$

$$P_X = [0.43 \quad 0.32 \quad 0.25], \text{ for } |\mathcal{S}| = 3. \quad (45)$$

Figure 6 illustrates the convergence of P_γ^* to the uniform distribution for different values of $|\mathcal{S}|$, again using the same initial distributions above for $|\mathcal{S}| = 2$ and $|\mathcal{S}| = 3$ and

$$P_X = [0.35 \quad 0.25 \quad 0.25 \quad 0.15], \text{ for } |\mathcal{S}| = 4. \quad (46)$$

4.2 The Three Bins Property

We wish to understand when P_γ^* ‘dominates’ P_X and vice versa. To this end, we define the sequence:

$$d_i = p_{(i)} - p_{(i)}^*, \quad i \in \mathbb{N}, \quad (47)$$

where $p_{(i)}$ is the i -th largest entry of P_X and $p_{(i)}^*$ is the i -th largest entry of P_γ^* in (18). By Corollary 1, P_X and P_γ^* share the same ordering; thus, d_i is well defined, preserving the correspondence between ordered entries. An immediate consequence of this and the fact that probabilities sum to one is the following lemma.

Lemma 1. *If P_X is uniform or $\gamma = 0$, then $d_i = 0$ for all $i \in \mathbb{N}$. Otherwise, the sequence $\{d_i\}$ has at least one sign change.*

Before providing the main result of this section, which can be thought of as a converse to Lemma 1, we present the following preparatory lemma.

Lemma 2. *For any fixed $\gamma > 0$, $\phi_\gamma(p) - \alpha_\gamma^* = 0$ has at least one and at most two roots. In particular,*

- $p_{\gamma,a} \in [0, p_\gamma^+)$ denotes the smallest root, which exists only if $\alpha_\gamma^* \geq 1$. For $\alpha_\gamma^* < 1$, we set $p_{\gamma,a} = 0$.
- $p_{\gamma,b} \in (p_\gamma^+, 1)$ denotes the largest root, which always exists.

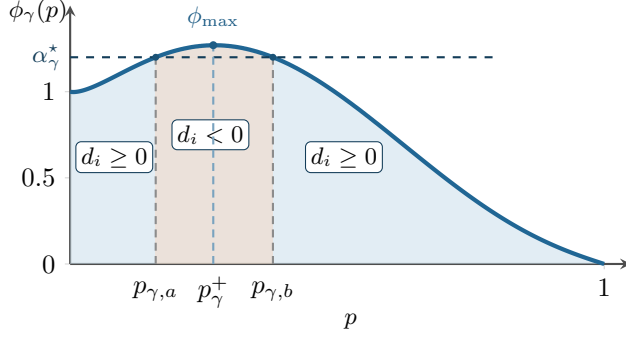


Figure 7: Illustration of Theorem 2.

Proof. We recall that $\phi_\gamma(p)$ is unimodal (Proposition 3); hence $\phi_\gamma(p) - \alpha_\gamma^* = 0$ has at most two roots. At least one root exists since

$$\alpha_\gamma^* \leq \max_{p \in (0,1)} \phi_\gamma(p), \quad (48)$$

as shown in Proposition 8. Moreover, since $\phi_\gamma(0^+) = 1$, $\phi_\gamma(1) = 0$, and ϕ_γ is unimodal, if $\alpha_\gamma^* < 1$ there is only one root, $p_{\gamma,b}$. This completes the proof. \square

The next result (proof in Appendix C.2) characterizes how the sequence of sign changes in $\{d_i\}$ behaves.

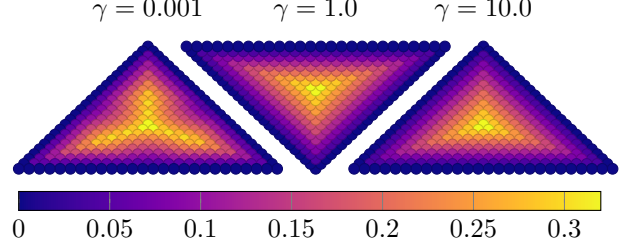
Theorem 2. *Suppose that P_X is not uniform and $\gamma > 0$. Then, the following holds:*

- if $p_{(i)} \in (0, p_{\gamma,a}]$, then $d_i \geq 0$;
- if $p_{(i)} \in (p_{\gamma,a}, p_{\gamma,b})$, then $d_i < 0$;
- if $p_{(i)} \in [p_{\gamma,b}, 1)$, then $d_i \geq 0$;

where $0 \leq p_{\gamma,a} \leq p_\gamma^+ \leq p_{\gamma,b} < 1$ are defined in Lemma 2.

Figure 7 illustrates the result in Theorem 2. In words, Theorem 2 has the following consequences:

- **Small-to-moderate probabilities** ($p_{\gamma,a}, p_{\gamma,b}$). In this regime $d_i < 0$ and hence, $p_{(i)}^* > p_{(i)}$. The focal-loss amplifies these probabilities, which is the principal mechanism by which it mitigates class imbalance, i.e., the probability mass is shifted toward mid-range entries.
- **Large probabilities** $[p_{\gamma,b}, 1)$. Here $d_i \geq 0$ and hence, $p_{(i)}^* \leq p_{(i)}$. The focal-loss downweights high-probability (“easy”) samples. Part of this effect is normalization: since mid-range probabilities are amplified and since $\sum_i p_{(i)}^* = 1$, then the largest entries must decrease.
- **Very small probabilities** $(0, p_{\gamma,a}]$. In this regime, which we refer to as *over-suppression regime*, we also have $d_i \geq 0$ and hence, $p_{(i)}^* \leq p_{(i)}$.


 Figure 8: Heatmap of $p_{\min} - p_{\gamma,a}$ over the ternary probability simplex.

Thus, extremely small probabilities are further suppressed, which can, in principle, exacerbate imbalance at the extreme tail. However, as shown in (13), for sufficiently large values of γ the interval $(0, p_{\gamma,a}]$ is empty or negligible. Thus, while in practice this effect is typically muted, one should not ignore this regime especially in extremely imbalanced regimes.

An immediate consequence of Theorem 2 is provided in the next corollary (see also Figure 7).

Corollary 2. *Suppose that P_X is not uniform and $\gamma > 0$. Then, the sequence $\{d_i\}, i \in \mathbb{N}$, has at least one and at most two sign changes.*

4.3 Sign Changes for Small Support Sizes

We show that when the support is binary (proof in Appendix C.3) and possibly ternary, we have $p_{\min} > p_{\gamma,a}$, i.e., the *over-suppression regime* never occurs.

Proposition 11. *Let $|\mathcal{S}| = 2$. Then, for all $\gamma > 0$, it holds that $d_1 \geq 0$ and $d_2 < 0$.*

Conjecture 1. *Let $|\mathcal{S}| = 3$. Then, for all $\gamma > 0$, it holds that $p_{\min} > p_{\gamma,a}$, i.e., $d_3 < 0$ (i.e., the *over-suppression regime* is absent for $|\mathcal{S}| = 3$).*

We now provide numerical and theoretical evidence in support of Conjecture 1. Numerically, we carried out extensive simulations (see Figure 8) and we could not find cases where $d_3 \geq 0$. To provide theoretical evidence, we use the next result (proof in Appendix C.4).

Proposition 12. *Let $|\mathcal{S}| = 3$. Then, for all $\gamma > 0$, it holds that $d_1 \geq 0$.*

Now, since $d_1 \geq 0$, two cases can occur:

1. $d_2 \geq 0$ (i.e., $p_{(2)} > p_{\gamma,b}$): in this case, from Corollary 2, we need $d_3 < 0$, i.e., $p_{\min} > p_{\gamma,a}$. Therefore, for this case, Conjecture 1 holds.
2. $d_2 < 0$ (i.e., $p_{\gamma,a} < p_{(2)} < p_{\gamma,b}$): For this regime, proving that $d_3 < 0$ (i.e., $p_{\min} > p_{\gamma,a}$) is an open problem. In other words, this is the only regime that must be addressed to prove Conjecture 1.

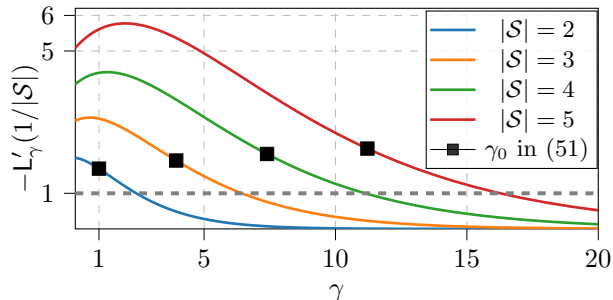


Figure 9: Illustration of conditions in (50) and (51).

Remark 5. Although for the case $|\mathcal{S}| \leq 3$ it appears that the *over-suppression regime* never occurs for all $\gamma > 0$, the same is not true for $|\mathcal{S}| \geq 4$. Appendix C.5 gives an example with $|\mathcal{S}| = 4$ where $p_{\min} < p_{\gamma,a}$.

4.4 Interplay between γ , Cardinality of the Support, and P_X

We now seek to study the interplay between γ , the cardinality of the support \mathcal{S} , and the values of P_X . In particular, we provide sufficient conditions under which the over-suppression regime does not exist.

Proposition 13. *Suppose that $|\mathcal{S}| < \infty$ and*

$$-p_{\max} L'_\gamma \left(\frac{1}{|\mathcal{S}|} \right) < 1. \quad (49)$$

Then, $p_{\gamma,a} = 0$, that is, the over-suppression regime does not exist.

Proof. Combining the upper bound on α_γ^* in (35) with the assumption in (49), we arrive at $\alpha_\gamma^* < 1$. By Lemma 2, $\alpha_\gamma^* < 1$ implies that $p_{\gamma,a} = 0$. This concludes the proof of Proposition 13. \square

The condition in (49) has three degrees of freedom, namely: p_{\max} , γ , and $|\mathcal{S}|$. This condition can be further loosened to

$$-L'_\gamma \left(\frac{1}{|\mathcal{S}|} \right) < 1. \quad (50)$$

From Figure 9, for each $|\mathcal{S}|$, there exists $\bar{\gamma}$, that depends only on $|\mathcal{S}|$, such that $p_{\gamma,a} = 0$ for all $\gamma > \bar{\gamma}$, i.e., eventually the over-suppression regime vanishes.

The next proposition (proof in Appendix C.6) provides an additional bound on the minimum value of γ that ensures that the over-suppression regime cannot occur.

Proposition 14. *Let $\kappa(\cdot)$ be given in (12). If $\gamma > \kappa(p_{\min})$, then $p_{\min} > p_{\gamma,a}$, that is, the over-suppression regime does not exist.*

We now present a final result giving a sufficient condition for $p_{\max} > p_{\gamma,b}$, i.e., $d_1 \geq 0$. In other words, the

next proposition (proof in Appendix C.7) ensures that the maximum probability is reduced.

Proposition 15. *Suppose that $|\mathcal{S}| < \infty$ and $\gamma > \gamma_0$ where*

$$\gamma_0 = -1 - \frac{1}{n} W_{-1}(-n \exp(-n)), \quad (51)$$

with $n = \log \left(\frac{|\mathcal{S}|}{|\mathcal{S}|-1} \right)$. Then, $p_{\max} > p_{\gamma,b}$, i.e., $d_1 > 0$.

Figure 9 also reports γ_0 from (51) for different values of $|\mathcal{S}|$. The condition $\gamma > \gamma_0$ in Proposition 15 is less stringent than (50), since the latter ensures both $d_1 \geq 0$ and $p_{\gamma,a} = 0$, while the former guarantees only $d_1 \geq 0$.

4.5 Majorization

It has been observed empirically (Mukhoti et al., 2020) that the focal-entropy optimizer P_γ^* typically has higher entropy than the original P_X . Here, we formalize this observation for distributions with finite support size, i.e., $|\mathcal{S}| < \infty$. We start with the following definition.

Definition 3 (Majorization). *For two vectors $x, y \in \mathbb{R}^n$, we say that x majorizes y (notation $x \succ y$) when*

$$\sum_{i=1}^k x_{(i)} \geq \sum_{i=1}^k y_{(i)}, \text{ for all } k = 1, \dots, n, \quad (52)$$

where $x_{(i)}$ is the i -th largest entry of x .

An immediate consequence of Theorem 2 is given in the next proposition (proof in Appendix C.8).

Proposition 16. *Suppose that $p_{\min} > p_{\gamma,a}$. Then, P_X majorizes P_γ^* , that is, $P_X \succ P_\gamma^*$.*

Note that sufficient conditions for which $p_{\min} > p_{\gamma,a}$ are provided in Proposition 13 and Proposition 14. Combining the result in Proposition 16 with Schur-convexity, we have the following consequences.

Corollary 3. *Suppose that $p_{\min} > p_{\gamma,a}$. Then:*

- Entropy increase:

$$H(P_\gamma^*) \geq H(P_X), \quad (53)$$

which follows since the Shannon entropy is Schur-concave (Kvålseth, 2022). The above result generalizes to the Rényi entropy (Kvålseth, 2022).

- Non-uniformity decrease: *By subtracting $\log(|\mathcal{S}|)$ from both sides of (53), we have that*

$$D_{\text{KL}}(P_X \| P_U) \geq D_{\text{KL}}(P_\gamma^* \| P_U), \quad (54)$$

where P_U is the uniform distribution.

Remark 6. Corollary 3 formalizes the empirical finding of (Mukhoti et al., 2020) that $H(P_\gamma^*) \geq H(P_X)$. This is significant, since higher-entropy predictions help reduce overconfidence (Mukhoti et al., 2020).

4.6 Relationship with Relative Entropy

We aim at relating the focal-entropy in (4) to the well-studied cross-entropy in (2). We start by noting that the focal-loss in Definition 1 can be equivalently written as

$$\mathsf{L}_\gamma(P_X(x)) = \mathsf{L}_0(P_X^{(\gamma)}(x)) - h_\gamma(P_X), \quad (55)$$

where

$$P_X^{(\gamma)}(x) = \frac{P_X(x)^{(1-P_X(x))^\gamma}}{\exp(h_\gamma(P_X))}, \quad (56)$$

and

$$h_\gamma(P_X) = \log \left(\sum_{x \in \mathcal{X}} P_X(x)^{(1-P_X(x))^\gamma} \right). \quad (57)$$

The function $h_\gamma(P_X)$ has recently appeared in other contexts, such as in a rate distortion framework with soft-reconstruction (Dytso and Cardone, 2025). The next lemma (proof in Appendix C.9) further tightens the upper bound presented in (Dytso and Cardone, 2025) and shows that the correction term $h_\gamma(P_X)$ is uniformly bounded.

Lemma 3. *Let $P_X \in \mathcal{P}(\mathcal{X})$. Then, for $\gamma \geq 0$, the two following properties hold:*

1. $\gamma \mapsto h_\gamma(P_X)$ is strictly increasing; and
2. $0 \leq h_\gamma(P_X) \leq e^{\frac{1}{e}} \gamma$.

The following proposition (proof in Appendix C.10) formalizes the connection between the focal-entropy and other information-theoretic quantities.

Proposition 17. *For any $P_X, Q_X \in \mathcal{P}(\mathcal{X})$ such that $P_X \ll Q_X$, it holds that*

$$H_\gamma(P_X, Q_X) = D_{\text{KL}}(P_X \| Q_X^{(\gamma)}) + H(P_X) - h_\gamma(Q_X) \quad (58)$$

$$= H_0(P_X, Q_X^{(\gamma)}) - h_\gamma(Q_X), \quad (59)$$

where $Q_X^{(\gamma)}$ and $h_\gamma(Q_X)$ are defined in (56) and in (57), respectively. Moreover, it holds that

$$H_\gamma(P_X, Q_X) = \rho_\gamma(P_X, Q_X) (D_{\text{KL}}(R_X \| Q_X) + H(R_X)), \quad (60)$$

where

$$R_X(x) = \frac{P_X(x)(1 - Q_X(x))^\gamma}{\rho_\gamma(P_X, Q_X)}, \quad (61)$$

and

$$\rho_\gamma(P_X, Q_X) = \mathbb{E}_{X \sim P_X} [(1 - Q_X(X))^\gamma]. \quad (62)$$

The next result (proof in Appendix C.11) leverages Lemma 3 and it establishes bounds on the difference between the minimum value of the cross-entropy and the minimum value of the focal-entropy.

Proposition 18. *Fix $\gamma \geq 0$. Then, it holds that*

$$0 \leq \inf_{Q_X} H(P_X, Q_X) - \inf_{Q_X} H_\gamma(P_X, Q_X) \leq e^{\frac{1}{e}} \gamma. \quad (63)$$

5 Experimental Validation

In this section, we validate our theoretical results on both *synthetic* and *real* data. For the synthetic case (Appendix D), we assume knowledge of the joint distribution over class labels and features, enabling direct theoretical validation.

For the *real* data, we used MNIST in binary classification: $C = 0$ for ‘digit is not 1’ and $C = 1$ for ‘digit is 1’, yielding class imbalance (53,258 of 60,000 images in class 0). From each 28×28 image, we extracted two zoning-style features capturing spatial asymmetry (Impedovo and Pirlo, 2014): F_1 , the intensity ratio of upper vs. lower halves, and F_2 , the intensity ratio of left vs. right halves. Each image was represented by these two features, which were then quantized into four bins (empirical quantiles (Dougherty et al., 1995)).

We trained a neural network (same architecture as in Appendix D) using the focal loss in (3) with $\gamma = 1$. The trained model estimated the probability of C for each of the 16 bin combinations (four bins for F_1 , four for F_2)—see the ‘Model $P_{C|F_1, F_2}$ ’ bars in Figure 10.

Since the true posterior is unknown, we approximated it by computing the empirical class proportions within each bin combination (‘Estimated $P_{C|F_1, F_2}$ ’ in Figure 10). Using this estimated posterior in (18), we derived P_γ^* for $\gamma = 1$ (‘Theory $P_{C|F_1, F_2}$ ’). Figure 10 shows that the network outputs closely match P_γ^* (maximum difference 0.017), supporting our theory and indicating convergence to the global minimum under focal loss.

6 Conclusion

We conducted a systematic study of properties of the focal-entropy. We showed that it preserves desirable features (finiteness and convexity), while also exhibiting behaviors that distinguish it fundamentally from the cross-entropy. We established the existence and uniqueness of its minimizer and described how it reshapes distributions by amplifying mid-range probabilities, suppressing large probability outcomes, and, under certain conditions, over-suppressing very small probabilities. This finding is particularly important for practitioners, as it highlights the need to carefully select γ to avoid the *over-suppressing* regime. These results clarify the trade-offs that the focal-loss introduces and provide a theoretical foundation for its use in imbalanced learning. We hope that this perspective

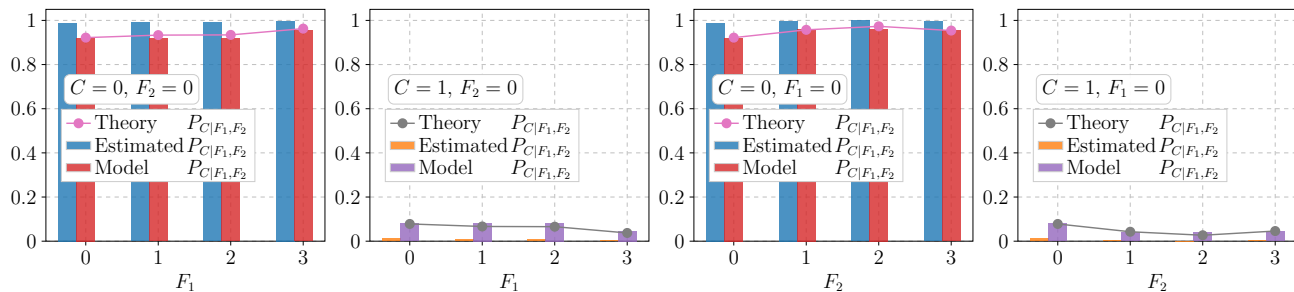


Figure 10: MNIST dataset: For each class, we fixed one of the features at its modal value and plotted: the true posterior, the posterior predicted by the trained neural network, and the theoretical focal-entropy minimizer. “Model $P_{C|F_1, F_2}$ ” denotes the predicted probability of class C for each of the 16 possible bin combinations (i.e., four bins for F_1 and four bins for F_2), which is estimated by using a neural network (see Appendix D for the architecture) trained by using the focal-loss in (3) with $\gamma = 1$; “Estimated $P_{C|F_1, F_2}$ ” refers to an empirical approximation of the posterior (since the true posterior is unknown), which is obtained by computing, for each of the 16 bin combinations, the proportion of samples with $C = 0$ and $C = 1$; and “Theory $P_{C|F_1, F_2}$ ” is the P_γ^* in (18) obtained by using “Estimated $P_{C|F_1, F_2}$ ” as input.

will guide both further theoretical developments and support more principled practical applications of the focal-loss. An interesting direction for future work is to investigate the potential benefits (if any) of the focal-loss in classification problems with soft, real-valued labels (Jeong et al., 2023).

A Proofs for Section 2

A.1 Proof of Proposition 1

To show the first property, note that for $p \in (0, 1)$, the function $\gamma \mapsto p^{(1-p)^\gamma}$ is strictly increasing and hence, $\gamma \mapsto L_\gamma(p)$ is strictly decreasing.

The first and second derivatives can be obtained through a straightforward calculation. It is also trivial to see that $L'_\gamma(p) < 0$ for all $p \in (0, 1)$ and $\gamma \geq 0$.

We now show that $L''_\gamma(p) > 0$ for all $p \in (0, 1)$ and $\gamma \geq 0$, which implies that $p \mapsto L_\gamma(p)$ is strictly convex on $(0, 1)$. We consider two cases separately:

- **Case $\gamma > 1$ or $\gamma = 0$:** it is trivial to see that the right-hand side of (9) is always positive;
- **Case $0 < \gamma \leq 1$:** by using the fact that $\log(p) \geq 1 - \frac{1}{p}$ for all $p > 0$, we can lower bound the second order derivative in (9) as follows,

$$L''_\gamma(p) \geq \frac{(1-p)^{\gamma-2}}{p^2} \left[\gamma(1-\gamma)p^2 \left(1 - \frac{1}{p}\right) + 2\gamma p(1-p) + (1-p)^2 \right] \quad (64)$$

$$= \frac{(1-p)^{\gamma-1}}{p^2} (\gamma^2 p + \gamma p + 1 - p), \quad (65)$$

which is always positive.

This concludes the proof of Proposition 1.

A.2 Proof of Proposition 2

The first property is directly derived from the inspection of (8).

For the second property, from (9), we have that $L''_\gamma(p) > 0$ on $p \in (0, 1)$. Thus, the function $p \mapsto L'_\gamma(p)$ is strictly increasing on $p \in (0, 1)$ and continuous. It therefore follows that $(L'_\gamma)^{-1}$ is also a strictly increasing function on its domain (i.e., the range of L'_γ), that is, $t \mapsto (L'_\gamma)^{-1}(t)$ is strictly increasing for $t < 0$.

Finally, the third property is a direct consequence of the first three properties.

This concludes the proof of Proposition 2.

A.3 Proof of Proposition 3

Property 1) follows by inspection.

To show Property 2), we start by proving that $p \mapsto \kappa(p)$ is strictly decreasing. By taking the first derivative of $\kappa(p)$ in (12), we obtain

$$\kappa'(p) = \frac{2p - 1 - \left(\log\left(\frac{1}{p}\right) - 1\right)^2}{p^2 \log^2\left(\frac{1}{p}\right)}. \quad (66)$$

The denominator is always positive and hence, we focus on studying the sign of the numerator, denoted as $f(p)$. We have that $f'(p) = \frac{2(p - \log(p) - 1)}{p} > 0$, where we have used $\log\left(\frac{1}{p}\right) > 1 - p$ for all $p \in (0, 1)$. Thus, $p \mapsto f(p)$ is strictly increasing, i.e., its maximum is $f(1) = 0$. It therefore follows that $f(p) < 0$ for all $p \in (0, 1)$ and hence, $\kappa'(p) < 0$ for all $p \in (0, 1)$, that is, $p \mapsto \kappa(p)$ is strictly decreasing.

We now prove that $\kappa(p) \leq 0$ for all $p \in [w, 1)$. Since $p \mapsto \kappa(p)$ is strictly decreasing, it suffices to show that $\kappa(w) = 0$. Setting (12) equal to zero, we arrive at

$$2p - \log(p) - 2 = 0, \quad (67)$$

or equivalently, after some manipulation,

$$(-2p) e^{-2p} = -2 e^{-2}, \quad (68)$$

which is satisfied for $p = w$ and $p = 1$.

Now, by using the first and second derivatives of L_γ in (8) and in (9), we have that

$$\phi'(p) = \gamma(1-p)^{\gamma-2} \left(\log\left(\frac{1}{p}\right) (1-\gamma p) - 2(1-p) \right) \quad (69)$$

$$= \gamma(1-p)^{\gamma-2} p \log\left(\frac{1}{p}\right) (\kappa(p) - \gamma), \quad (70)$$

which implies that the above derivative is negative whenever $\gamma > \kappa(p)$ and positive if $\gamma < \kappa(p)$.

To show Property 3), note that

$$\phi_\gamma(p) = p(1-p)^{\gamma-1} \left(\gamma \log \frac{1}{p} + \frac{1-p}{p} \right) \quad (71)$$

$$\leq (1-p)^\gamma (1+\gamma) \quad (72)$$

$$\leq 1 + \gamma, \quad (73)$$

where (72) follow by using the bound $\log x \leq x - 1$, $x > 0$.

We now show Property 4). To show the first upper bound, note that by Property 2), $\phi_\gamma(p)$ is decreasing on $p \in [w, 1)$ since $\kappa(p) < 0$. Hence, $p_\gamma^+ \leq w$.

The second upper bound follows by noting that p_γ^+ is such that $\kappa(p_\gamma^+) = \gamma$, which implies that

$$\frac{1}{p_\gamma^+} - \frac{2(1-p_\gamma^+)}{p_\gamma^+ \log\left(\frac{1}{p_\gamma^+}\right)} = \gamma. \quad (74)$$

By using the change of variable $p_\gamma^+ = e^{-x}$, $x > 0$, we can rewrite the above as follows,

$$\gamma = e^x - \frac{2(e^x - 1)}{x} \leq e^x - 2e^{\frac{x}{2}}, \quad (75)$$

where the inequality follows since $\frac{e^x - 1}{x} \geq e^{\frac{x}{2}}$ for $x > 0$. By letting $y = e^{\frac{x}{2}}$, the above inequality can be rewritten as

$$y^2 - 2y - \gamma \geq 0, \quad (76)$$

which, since $\gamma \geq 0$, implies that

$$y \geq 1 + \sqrt{1 + \gamma}, \quad (77)$$

and hence, proves the upper bound on p_γ^+ .

To show Property 5), we use (11) and write

$$\frac{\phi_\gamma(u)}{\phi_\gamma\left(\frac{1-u}{2}\right)} = \frac{(1-u)^\gamma \left(\gamma \frac{1-u}{1-u} \log\left(\frac{1}{u}\right) + 1 \right)}{\left(\frac{1+u}{2}\right)^\gamma \left(\gamma \frac{1-u}{1+u} \log\left(\frac{2}{1-u}\right) + 1 \right)} \quad (78)$$

$$= \left(\frac{2}{s_u}\right)^\gamma \left(\frac{1 + \gamma \frac{\log(1+t_u)}{t_u}}{1 + \gamma \frac{\log(1+s_u)}{s_u}} \right), \quad (79)$$

where we let $t_u = \frac{1-u}{u}$ and $s_u = \frac{1+u}{1-u}$. By leveraging the equality above and letting $T_u = \frac{\log(1+t_u)}{t_u}$ and $S_u = \frac{\log(1+s_u)}{s_u}$, we can write

$$\phi_\gamma(u) - \phi_\gamma\left(\frac{1-u}{2}\right) = \frac{\phi_\gamma\left(\frac{1-u}{2}\right)}{1 + \gamma S_u} \left[\left(\frac{2}{s_u}\right)^\gamma (1 + \gamma T_u) - (1 + \gamma S_u) \right]. \quad (80)$$

Our goal is to prove that the above expression is non-negative for all $u \in (0, 1/3]$. We note that from Property 1) and the fact that $S_u > 0$, we have that $\frac{\phi_\gamma(\frac{1-u}{2})}{1+\gamma S_u} \geq 0$. Thus, proving that (80) is non-negative for all $u \in (0, 1/3]$ is equivalent to prove that

$$f_u(\gamma) = \left(\frac{2}{s_u}\right)^\gamma (1 + \gamma T_u) - (1 + \gamma S_u) \quad (81)$$

is non-negative for all $u \in (0, 1/3]$. We next prove that this is the case by showing that $\gamma \mapsto f_u(\gamma)$ is non-decreasing for all $u \in (0, 1/3]$, which implies that

$$f_u(\gamma) \geq f_u(0) = 0, \quad (82)$$

for all $u \in (0, 1/3]$. To show that $\gamma \mapsto f_u(\gamma)$ in (81) is non-decreasing for all $u \in (0, 1/3]$, it suffices to show that $f'_u(\gamma) \geq 0$ for all $u \in (0, 1/3]$. To prove this, we first show that $\gamma \mapsto f'_u(\gamma)$ is strictly increasing and then show that $f'_u(0) \geq 0$ for all $u \in (0, 1/3]$.

We have that

$$f'_u(\gamma) = \log\left(\frac{2}{s_u}\right) \left(\frac{2}{s_u}\right)^\gamma (1 + \gamma T_u) + \left(\frac{2}{s_u}\right)^\gamma T_u - S_u, \quad (83)$$

and

$$f''_u(\gamma) = \left(\frac{2}{s_u}\right)^\gamma \log\left(\frac{2}{s_u}\right) \left[\log\left(\frac{2}{s_u}\right) (1 + \gamma T_u) + 2T_u \right]. \quad (84)$$

Now, since $s_u \leq 2$ and $T_u > 0$ for all $u \in (0, 1/3]$, it follows that $f''_u(\gamma) > 0$ for all $u \in (0, 1/3]$. Thus, $\gamma \mapsto f'_u(\gamma)$ is strictly increasing for all $u \in (0, 1/3]$.

We now show that, for all $u \in (0, 1/3]$, it holds that $f'_u(0) \geq 0$. We have that

$$f'_u(0) = \log\left(\frac{2}{s_u}\right) + T_u - S_u \quad (85)$$

$$= \log\left(\frac{2}{s_u}\right) + \frac{\log(1+t_u)}{t_u} - \frac{\log(1+s_u)}{s_u} \quad (86)$$

$$= \frac{1}{(1-u^2)} (2u(1-u) \log(2) - (1-u^2) \log(1+u) + 2(1-u) \log(1-u) - u(1+u) \log(u)), \quad (87)$$

where the last equality follows by substituting the definitions of t_u and s_u . Note that the denominator of $f'_u(0)$ is always positive for all $u \in (0, 1/3]$. Therefore, to prove $f'_u(0) \geq 0$ for all $u \in (0, 1/3]$, it suffices to prove that the numerator of (87) is non-negative for all $u \in (0, 1/3]$. We denote the numerator of (87) by $g_u(0)$. In what follows, we will show that, for all $u \in (0, 1/3]$, we have that $g_u(0)$ is concave and hence, it achieves minimum value at one of its end points, which are

$$g_{0+}(0) = g_{1/3}(0) = 0. \quad (88)$$

To prove concavity, we take the second derivative of $g_u(0)$. It is a simple exercise to obtain

$$\frac{d^2}{du^2} g_u(0) = \frac{1 - 5u^2 - 2u(1-u^2) \log\left(\frac{1+u}{4u}\right)}{u(u^2-1)}. \quad (89)$$

For all $u \in (0, 1/3]$, the denominator of the above expression is always negative and hence, to prove concavity of $g_u(0)$ it suffices to prove that the numerator of (89) is positive for all $u \in (0, 1/3]$. We denote the numerator of (89) by $h_u(0)$. We have that

$$h_u(0) = 1 - 5u^2 - 2u(1-u^2) \log\left(\frac{1+u}{4u}\right) \quad (90)$$

$$\geq 1 - 5u^2 - 2u(1-u^2) \left(\frac{1+u}{4u} - 1\right) \quad (91)$$

$$= \frac{1}{2}(1 + 3u - 9u^2 - 3u^3) \quad (92)$$

$$= \frac{1}{2}((1 - 9u^2) + 3u(1 - u^2)) \quad (93)$$

$$> 0, \tag{94}$$

where the first inequality follows by using the fact that $\log(x) \leq x - 1$ for all $x > 0$ and the second inequality is due to the fact that, for all $u \in (0, 1/3]$, we have that $(1 - 9u^2) \geq 0$ and $3u(1 - u^2) > 0$. Thus, for all $u \in (0, 1/3]$, $h_u(0) > 0$, which implies that $g_u(0)$ is concave with $g_u(0) \geq 0$ and hence, $f'_u(0) \geq 0$, concluding the proof that $\gamma \mapsto f_u(\gamma)$ in (81) is non-decreasing for all $u \in (0, 1/3]$. This concludes the proof of Proposition 3.

B Proofs for Section 3

B.1 Additional Properties of the Mapping $\gamma \mapsto H_\gamma(P_X, Q_X)$

Consider the mapping $\gamma \mapsto H_\gamma(P_X, Q_X)$. The first and second order derivatives are given by

$$\frac{d}{d\gamma} H_\gamma(P_X, Q_X) = \mathbb{E} [\log(1 - Q_X(X)) L_\gamma(Q_X(X))] \leq 0, \tag{95}$$

$$\frac{d^2}{d\gamma^2} H_\gamma(P_X, Q_X) = \mathbb{E} \left[(\log(1 - Q_X(X)))^2 L_\gamma(Q_X(X)) \right] \geq 0, \tag{96}$$

where the expectations are taken with respect to $X \sim P_X$.

B.2 Proof of Proposition 5

Define a positive measure

$$\mu(x) = P_X(x) \log \frac{1}{Q_X(x)}, \quad x \in \mathcal{X}, \tag{97}$$

which is well-defined, in view of the fact that $P_X \ll Q_X$, and has the same support as P_X , namely \mathcal{S} . Moreover, μ is a finite measure since, from (2), we have that

$$\sum_x \mu(x) = H(P_X, Q_X) < \infty, \tag{98}$$

where the inequality holds from the assumption. Next, note that we can write

$$\begin{aligned} H_\gamma^{\frac{1}{\gamma}}(P_X, Q_X) &= \left(\sum_x \mu(x) (1 - Q_X(x))^\gamma \right)^{\frac{1}{\gamma}} \\ &= \|1 - Q_X(\cdot)\|_\gamma, \end{aligned} \tag{99}$$

where $\|\cdot\|_p$ is the $\ell_p(\mathcal{X}, \mu)$, $p > 0$, norm. Now, taking the limit for $\gamma \rightarrow \infty$ and using the standard result that ℓ_p norms converge to the essential supremum of the underlying function (Folland, 1999, Ch. 6, Ex. 7), we arrive at

$$\lim_{\gamma \rightarrow \infty} \|1 - Q_X(\cdot)\|_\gamma = \sup_{x \in \text{support } \mu} (1 - Q_X(x)) \tag{100}$$

$$= \sup_{x \in \mathcal{S}} (1 - Q_X(x)), \tag{101}$$

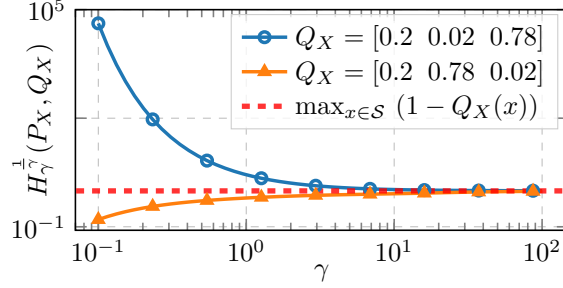
where in the last step we have used the fact that μ is supported on \mathcal{S} . The proof of Proposition 5 is concluded by noting that (101) is equal to one if \mathcal{S} is countably infinite.

Figure 11 provides an illustration of the convergence of $H_\gamma^{\frac{1}{\gamma}}(P_X, Q_X)$ for a fixed P_X with $|\mathcal{S}| = 3$ and two different distributions Q_X . From Figure 11, we note that this convergence is pretty fast.

B.3 Proof of Proposition 6

If P_X is not absolutely continuous with respect to Q_X , the statement trivially holds by the definition in (4). Hence, suppose that $P_X \ll Q_X$. Then, on the one hand, from Proposition 4, we have that

$$H_\gamma(P_X, Q_X) \leq H(P_X, Q_X). \tag{102}$$


 Figure 11: $P_X = [0.4 \ 0.58 \ 0.02]$.

On the other hand, fix some $\delta > 0$ and let $\mathcal{Q}_\delta = \{x \in \mathcal{X} : Q_X(x) \leq \delta\}$. Then,

$$\begin{aligned} H_\gamma(P_X, Q_X) &\geq \sum_{x \in \mathcal{Q}_\delta} P_X(x) (1 - Q_X(x))^\gamma \log \left(\frac{1}{Q_X(x)} \right) \\ &\geq (1 - \delta)^\gamma \sum_{x \in \mathcal{Q}_\delta} P_X(x) \log \left(\frac{1}{Q_X(x)} \right) \end{aligned} \quad (103)$$

$$= (1 - \delta)^\gamma (H(P_X, Q_X) - \Delta_\delta), \quad (104)$$

where we have defined

$$\Delta_\delta = \sum_{x \in \mathcal{Q}_\delta^c} P_X(x) \log \left(\frac{1}{Q_X(x)} \right). \quad (105)$$

Next, note that since \mathcal{Q}_δ^c is a finite set, then Δ_δ is a finite sum for all $\delta > 0$. Combining (102) and (104), we conclude that $H_\gamma(P_X, Q_X) < \infty$ if and only if $H(P_X, Q_X) < \infty$, which concludes the proof of Proposition 6.

B.4 Proof of Proposition 7

Consider a sequence Q_n that converges to a distribution Q_∞ . Then, the lower semicontinuity property follows from the application of Fatou's lemma since

$$\liminf_{n \rightarrow \infty} H_\gamma(P_X, Q_n) \geq \mathbb{E} \left[\liminf_{n \rightarrow \infty} L_\gamma(Q_n(X)) \right] \quad (106)$$

$$= H_\gamma(P_X, Q_\infty). \quad (107)$$

To show the convexity property, recall from Proposition 1 that $p \mapsto L_\gamma(p)$ is strictly convex on $(0, 1)$ for $\gamma \geq 0$. Consequently,

$$H_\gamma(P_X, Q) = \sum_{x \in \mathcal{X}} P_X(x) L_\gamma(Q(x)) \quad (108)$$

is a non-negative weighted sum of strictly convex functions and hence, it is convex in Q . Moreover, $H_\gamma(P_X, Q)$ is strictly convex in Q on \mathcal{S} due to the fact that it is a positive weighted sum of strictly convex functions. This concludes the proof of Proposition 7.

B.5 Proof of Corollary 1

Property 1) follows directly from the expression of P_γ^* in (18).

For Property 2), note that the fact that $P_X(x_1) \geq P_X(x_2)$ implies that

$$-\frac{\alpha_\gamma^*}{P_X(x_1)} \geq -\frac{\alpha_\gamma^*}{P_X(x_2)}. \quad (109)$$

By applying $(L'_\gamma)^{-1}$ to both sides of the above inequality and recalling that $t \mapsto (L'_\gamma)^{-1}(t)$ for $t \in (-\infty, 0)$ is strictly increasing (see Proposition 2), we arrive at

$$P_\gamma^*(x_1) \geq P_\gamma^*(x_2). \quad (110)$$

For Property 3), note that to have $P_\gamma^* = P_X$, from (18) we would, in fact, need that

$$(\mathbf{L}'_\gamma)^{-1} \left(-\frac{\alpha_\gamma^*}{P_X(x)} \right) = P_X(x) \text{ for all } x \in \mathcal{S}, \quad (111)$$

or equivalently

$$\alpha_\gamma^* = -P_X(x) \mathbf{L}'_\gamma(P_X(x)), \text{ for all } x \in \mathcal{S}. \quad (112)$$

Since the function $p \mapsto \mathbf{L}'_\gamma(p)$ is strictly increasing on $p \in (0, 1)$ and continuous (see Proposition 1), then the above equation is satisfied if and only if $\gamma = 0$ or P_X is a uniform distribution.

This concludes the proof of Corollary 1.

B.6 Proof of Proposition 8

We start by showing (34). Toward this end, let $\phi_{\gamma, M} = \max_{t \in (0, 1)} \phi_\gamma(t)$ and let

$$q_i = (\mathbf{L}'_\gamma)^{-1} \left(-\frac{\phi_{\gamma, M}}{p_i} \right), \quad (113)$$

from which we obtain

$$p_i = -\frac{\phi_{\gamma, M}}{\mathbf{L}'_\gamma(q_i)} = \frac{\phi_{\gamma, M}}{\phi_\gamma(q_i)} q_i \geq q_i, \quad (114)$$

for all i 's. Thus, we have that

$$F(\phi_{\gamma, M}) = \sum_i (\mathbf{L}'_\gamma)^{-1} \left(-\frac{\phi_{\gamma, M}}{p_i} \right) = \sum_i q_i \leq \sum_i p_i = 1. \quad (115)$$

Since $\alpha \mapsto F(\alpha)$ is strictly decreasing and $F(\alpha_\gamma^*) = 1$, it follows that $\alpha_\gamma^* \leq \phi_{\gamma, M}$. Finally, the bound $\phi_{\gamma, M} \leq 1 + \gamma$ is given in Proposition 3.

We now show (35). From the definition of α_γ^* , we have that

$$\frac{1}{N} = \frac{1}{N} \sum_{x \in \mathcal{S}} (\mathbf{L}'_\gamma)^{-1} \left(-\frac{\alpha_\gamma^*}{P_X(x)} \right), \quad (116)$$

and an additional note that

$$\begin{aligned} (\mathbf{L}'_\gamma)^{-1} \left(-\frac{\alpha_\gamma^*}{p_{\min}} \right) &\leq \frac{1}{N} \sum_{x \in \mathcal{S}} (\mathbf{L}'_\gamma)^{-1} \left(-\frac{\alpha_\gamma^*}{P_X(x)} \right) \\ &\leq (\mathbf{L}'_\gamma)^{-1} \left(-\frac{\alpha_\gamma^*}{p_{\max}} \right), \end{aligned} \quad (117)$$

where the inequalities follow from the fact that $t \mapsto (\mathbf{L}'_\gamma)^{-1}(t)$ for $t \in (-\infty, 0)$ is strictly increasing, as shown in Proposition 2. Now, using the fact that $p \mapsto \mathbf{L}'_\gamma(p)$ is strictly increasing on $p \in (0, 1)$, as shown in Proposition 1, and applying it to (116) and (117) we arrive at

$$-\frac{\alpha_\gamma^*}{p_{\min}} \leq \mathbf{L}'_\gamma \left(\frac{1}{N} \right) \leq -\frac{\alpha_\gamma^*}{p_{\max}}, \quad (118)$$

which leads to (35).

We now prove (36). Let $p_{(i)}$ denote the i th largest entry of P_X . Under the assumption $\gamma > \kappa(p_{\min})$, we know from Proposition 3 that $\phi(\cdot)$ is strictly decreasing, i.e.,

$$\phi(p_{(1)}) < \cdots < \phi(p_{(N)}), \quad (119)$$

which, for all $i \in \{1, \dots, N\}$, implies that

$$-\frac{\phi(p_{(1)})}{p_{(i)}} > -\frac{\phi(p_{(i)})}{p_{(i)}} = \mathbf{L}'_\gamma(p_{(i)}). \quad (120)$$

Now, by applying $(L'_\gamma)^{-1}$ on both sides of the above inequality and recalling that $t \mapsto (L'_\gamma)^{-1}(t)$ for $t \in (-\infty, 0)$ is strictly increasing (see Proposition 2), we get

$$p_{(i)} < (L'_\gamma)^{-1} \left(-\frac{\phi(p_{(1)})}{p_{(i)}} \right). \quad (121)$$

Similarly, for all $i \in \{1, \dots, N\}$, we conclude that

$$p_{(i)} > (L'_\gamma)^{-1} \left(-\frac{\phi(p_{(N)})}{p_{(i)}} \right). \quad (122)$$

Now, evaluating $F(\cdot)$ in (21) in $\phi(p_{(1)})$, we obtain

$$F(\phi(p_{(1)})) = \sum_{i=1}^N (L'_\gamma)^{-1} \left(-\frac{\phi(p_{(1)})}{p_{(i)}} \right) > \sum_{i=1}^N p_{(i)} = 1, \quad (123)$$

and evaluating $F(\cdot)$ in (21) in $\phi(p_{(N)})$, we obtain

$$F(\phi(p_{(N)})) = \sum_{i=1}^N (L'_\gamma)^{-1} \left(-\frac{\phi(p_{(N)})}{p_{(i)}} \right) < \sum_{i=1}^N p_{(i)} = 1. \quad (124)$$

Now recall that $F(\alpha)$ is continuous and strictly decreasing in α . Thus, by monotonicity, we conclude the proof of (36). The proof of (37) follows by the same steps as those used for the proof of (36) with the only difference that, under the assumption $\gamma < \kappa(p_{\max})$, we know from Proposition 3 that $\phi(\cdot)$ is now strictly increasing, i.e.,

$$\phi(p_{(1)}) > \dots > \phi(p_{(N)}), \quad (125)$$

This concludes the proof of Proposition 8.

B.7 Proof of Proposition 9

From Proposition 7, we have that the mapping $Q_X \mapsto H_\gamma(P_X, Q_X)$ is strictly convex on $\{0, 1\}$ provided that the distribution P_X is non-degenerate. Thus, by letting $q = Q_X(1)$ (or equivalently, $Q_X(0) = 1 - q$), the derivative

$$D(q) = \frac{d}{dq} H_\gamma(P_X, \{q, 1 - q\}) \quad (126)$$

$$= p(1 - q)^{\gamma-1} \left(\gamma \log(q) - \frac{1 - q}{q} \right) + (1 - p)q^{\gamma-1} \left(-\gamma \log(1 - q) + \frac{q}{1 - q} \right) \quad (127)$$

is strictly increasing with a unique root q_γ^* . Note also that the fact that $p \in (0, \frac{1}{2}]$ from (40) implies that $q_\gamma \leq \frac{1}{2}$ for all $\gamma > 0$.

We prove lower bound in (39). From (40), we have that

$$\frac{q_\gamma}{1 - q_\gamma} = \frac{p^{\frac{1}{\gamma}}}{p^{\frac{1}{\gamma}} + (1 - p)^{\frac{1}{\gamma}}} \frac{p^{\frac{1}{\gamma}} + (1 - p)^{\frac{1}{\gamma}}}{(1 - p)^{\frac{1}{\gamma}}} = \frac{p^{\frac{1}{\gamma}}}{(1 - p)^{\frac{1}{\gamma}}}, \quad (128)$$

or equivalently

$$\frac{1 - p}{p} = \left(\frac{1 - q_\gamma}{q_\gamma} \right)^\gamma. \quad (129)$$

Using the above inside (127), we obtain

$$D(q_\gamma) = p \frac{(1 - q_\gamma)^{\gamma-1}}{q_\gamma} [\gamma \Delta(q_\gamma) + 2q_\gamma - 1], \quad (130)$$

where $\Delta(q) = (1 - q) \log\left(\frac{1}{1-q}\right) - q \log\left(\frac{1}{q}\right) \leq 0$ for $q \leq \frac{1}{2}$. Thus, since $q_\gamma \leq \frac{1}{2}$, we have that

$$D(q_\gamma) \leq p \frac{(1 - q_\gamma)^{\gamma-1}}{q_\gamma} (2q_\gamma - 1) \leq 0, \quad (131)$$

which implies that $q_\gamma \leq q_\gamma^*$.

We now prove the upper bound in (39). From (40), we have that

$$\frac{1-p}{p} = \left(\frac{1-q_{\gamma+1}}{q_{\gamma+1}}\right)^{\gamma+1}. \quad (132)$$

Using the above inside (127), we obtain

$$D(q_{\gamma+1}) = \gamma p \frac{(1 - q_{\gamma+1})^{\gamma-1}}{q_{\gamma+1}^2} \left[(1 - q_{\gamma+1})^2 \log\left(\frac{1}{1-q_{\gamma+1}}\right) - q_{\gamma+1}^2 \log\left(\frac{1}{q_{\gamma+1}}\right) \right]. \quad (133)$$

For $q \leq \frac{1}{2}$, we have that $(1 - q)^2 \log\left(\frac{1}{1-q}\right) \geq q^2 \log\left(\frac{1}{q}\right)$ and hence, $D(q_{\gamma+1}) \geq 0$, leading to $q_\gamma^* \leq q_{\gamma+1}$.

Combining the fact that $D(q_\gamma) \leq 0 \leq D(q_{\gamma+1})$ with the strict monotonicity of D yields

$$q_\gamma \leq q_\gamma^* \leq q_{\gamma+1}. \quad (134)$$

We now prove (41). By the mean value theorem, there exists $\xi \in (\gamma, \gamma + 1)$ such that

$$q'(\xi) = q_{\gamma+1} - q_\gamma = \tilde{Q}_{\gamma+1}(1) - \tilde{Q}_\gamma(1), \quad (135)$$

where $q'(\xi) = \frac{d}{d\gamma} q_\gamma \Big|_{\gamma=\xi}$, which can be computed from (40), that is,

$$q'(\xi) = -\log\left(\frac{p}{1-p}\right) \frac{q_\xi(1 - q_\xi)}{\xi^2} \quad (136)$$

$$\leq \left| \log\left(\frac{p}{1-p}\right) \right| \frac{1}{4\xi^2} \quad (137)$$

$$\leq \left| \log\left(\frac{p}{1-p}\right) \right| \frac{1}{4\gamma^2}, \quad (138)$$

where (137) follows since $q_\gamma(1 - q_\gamma) \leq \frac{1}{4}$ for $q_\gamma \leq \frac{1}{2}$ and (138) follows since $\xi \in (\gamma, \gamma + 1)$. Combining (135) with (138), we arrive at

$$\tilde{Q}_{\gamma+1}(1) - \tilde{Q}_\gamma(1) \leq \left| \log\left(\frac{p}{1-p}\right) \right| \frac{1}{4\gamma^2}. \quad (139)$$

This concludes the proof of Proposition 9.

C Proofs for Section 4

C.1 Proof of Proposition 10

Let f_0 be such that $(L'_\gamma)^{-1}(f_0) = \frac{1}{|\mathcal{S}|}$. Then, using the Taylor remainder theorem, we have that

$$P_\gamma^*(x) = (L'_\gamma)^{-1} \left(-\frac{\alpha_\gamma^*}{P_X(x)} \right) \quad (140)$$

$$= \frac{1}{|\mathcal{S}|} - \left(\frac{\alpha_\gamma^*}{P_X(x)} + f_0 \right) \frac{d}{dt} (L'_\gamma)^{-1}(t) \Big|_{t=f_0} + R_{x,\infty} \quad (141)$$

$$= \frac{1}{|\mathcal{S}|} - \frac{\left(\frac{\alpha_\gamma^*}{P_X(x)} + f_0 \right)}{L''_\gamma((L'_\gamma)^{-1}(f_0))} + R_{x,\infty} \quad (142)$$

$$= \frac{1}{|\mathcal{S}|} - \frac{\left(\frac{\alpha_\gamma^*}{P_X(x)} + \mathbf{L}'_\gamma\left(\frac{1}{|\mathcal{S}|}\right)\right)}{\mathbf{L}''_\gamma\left(\frac{1}{|\mathcal{S}|}\right)} + R_{x,\infty}, \quad (143)$$

where the last step follows from the fact that $f_0 = \mathbf{L}'_\gamma\left(\frac{1}{|\mathcal{S}|}\right)$ and the remainder term is given by

$$R_{x,\infty} = \frac{\left(\frac{\alpha_\gamma^*}{P_X(x)} + \mathbf{L}'_\gamma\left(\frac{1}{|\mathcal{S}|}\right)\right)^2}{2} \frac{d^2(\mathbf{L}'_\gamma)^{-1}(t)}{dt^2} \Big|_{t=c} \quad (144)$$

$$= -\frac{\left(\frac{\alpha_\gamma^*}{P_X(x)} + \mathbf{L}'_\gamma\left(\frac{1}{|\mathcal{S}|}\right)\right)^2}{2} \frac{\mathbf{L}'''_\gamma(u)}{(\mathbf{L}''_\gamma(u))^3} \Big|_{u=(\mathbf{L}'_\gamma)^{-1}(c)}, \quad (145)$$

for some $c \in \left(\mathbf{L}'_\gamma\left(\frac{1}{|\mathcal{S}|}\right), -\frac{\alpha_\gamma^*}{P_X(x)}\right)$. By combining the bounds on α_γ^* in (35), it is not difficult to see that

$$R_{x,\infty} = O\left(\frac{1}{\gamma}\right). \quad (146)$$

Summing both sides of (143) over $x \in \mathcal{S}$, we arrive at

$$\alpha_\gamma^* \sum_{x \in \mathcal{S}} \frac{1}{P_X(x)} + |\mathcal{S}| \mathbf{L}'_\gamma\left(\frac{1}{|\mathcal{S}|}\right) - \mathbf{L}''_\gamma\left(\frac{1}{|\mathcal{S}|}\right) \sum_{x \in \mathcal{S}} R_{x,\infty} = 0, \quad (147)$$

which implies that

$$\alpha_\gamma^* = -\mathbf{L}'_\gamma\left(\frac{1}{|\mathcal{S}|}\right) \text{HM}(P_X) + \frac{\text{HM}(P_X)}{|\mathcal{S}|} \mathbf{L}''_\gamma\left(\frac{1}{|\mathcal{S}|}\right) \sum_{x \in \mathcal{S}} R_{x,\infty} \quad (148)$$

$$= -\mathbf{L}'_\gamma\left(\frac{1}{|\mathcal{S}|}\right) \text{HM}(P_X) + O\left(\gamma \left(1 - \frac{1}{|\mathcal{S}|}\right)^\gamma\right), \quad (149)$$

where the last step follows by using (146).

Now, inserting (149) into (143), we arrive at the conclusion that as $\gamma \rightarrow \infty$, we have that

$$P_\gamma^*(x) = \frac{1}{|\mathcal{S}|} + \frac{\mathbf{L}'_\gamma\left(\frac{1}{|\mathcal{S}|}\right)}{\mathbf{L}''_\gamma\left(\frac{1}{|\mathcal{S}|}\right)} \left(\frac{\text{HM}(P_X)}{P_X(x)} - 1\right) + O\left(\frac{1}{\gamma}\right) \quad (150)$$

$$= \frac{1}{|\mathcal{S}|} + O\left(\frac{1}{\gamma}\right), \quad (151)$$

where in the last equality we have used that $\frac{\mathbf{L}'_\gamma\left(\frac{1}{|\mathcal{S}|}\right)}{\mathbf{L}''_\gamma\left(\frac{1}{|\mathcal{S}|}\right)} = O\left(\frac{1}{\gamma}\right)$. This concludes the proof of Proposition 10.

C.2 Proof of Theorem 2

We consider two cases:

Case 1: If $p_{(i)} \in (0, p_{\gamma,a}]$ or $p_{(i)} \in [p_{\gamma,b}, 1)$, then $\alpha_\gamma^* \geq \phi_\gamma(p_{(i)})$. Since $t \mapsto (\mathbf{L}'_\gamma)^{-1}(t)$ for $t \in (-\infty, 0)$ is strictly increasing (see Proposition 2), we have that

$$p_{(i)} \geq (\mathbf{L}'_\gamma)^{-1}\left(-\frac{\alpha_\gamma^*}{p_{(i)}}\right). \quad (152)$$

From (18), the right-hand side of the above inequality is precisely $p_{(i)}^*$ and hence, $d_i \geq 0$.

Case 2: If $p_{(i)} \in (p_{\gamma,a}, p_{\gamma,b})$, then $\alpha_\gamma^* < \phi_\gamma(p_{(i)})$. Since $t \mapsto (\mathbf{L}'_\gamma)^{-1}(t)$ for $t \in (-\infty, 0)$ is strictly increasing (see Proposition 2), this implies that

$$p_{(i)} < (\mathbf{L}'_\gamma)^{-1}\left(-\frac{\alpha_\gamma^*}{p_{(i)}}\right). \quad (153)$$

From (18), the right-hand side of the above inequality is precisely $p_{(i)}^*$ and hence, $d_i < 0$. This concludes the proof of Theorem 2.

C.3 Proof of Proposition 11

We focus on the case $\alpha_\gamma^* \geq 1$ (if $\alpha_\gamma^* < 1$, then from Lemma 2, the result trivially holds). If $\alpha_\gamma^* \geq 1$, then we need $\alpha_\gamma^* = \phi_\gamma(p_{\gamma,b}) \geq 1$. However, we now prove that for all $p \in [1/2, 1)$, we have that $\phi_\gamma(p) < 1$, which implies that $p_{\gamma,b} < 1/2$ (to ensure that $\phi_\gamma(p_{\gamma,b}) \geq 1$) and hence, $p_{(1)} > p_{\gamma,b}$, i.e., $d_1 \geq 0$. The fact that $\phi_\gamma(p) < 1$, for all $p \in [1/2, 1)$ is because: (i) from Proposition 3, $\phi_\gamma(p)$ is unimodal and it is such that $\phi_\gamma(0^+) = 1$ and $\phi_\gamma(1) = 0$; (ii) $\phi_\gamma(1/2) < 1$; (iii) $p \mapsto \phi_\gamma(p)$ is strictly decreasing on $p \in [1/2, 1)$ (from Proposition 3). Thus, $p_{\max} \geq p_{\gamma,b}$, i.e., $d_1 \geq 0$. The fact that $d_2 < 0$ follows from Corollary 2. This concludes the proof of Proposition 11.

C.4 Proof of Proposition 12

From Proposition 3, since $p_{\gamma,a} < 1/3$, we have that

$$\phi_\gamma(p_{\gamma,a}) > \phi_\gamma\left(\frac{1-p_{\gamma,a}}{2}\right). \quad (154)$$

Moreover, we also need

$$\alpha_\gamma^* = \phi_\gamma(p_{\gamma,a}) = \phi_\gamma(p_{\gamma,b}). \quad (155)$$

The above two equations, together with the unimodality of ϕ_γ (see Proposition 3), imply that

$$p_{\gamma,b} < \frac{1-p_{\gamma,a}}{2}. \quad (156)$$

We are now ready to prove that $d_1 \geq 0$. The proof is by contradiction. Assume that $d_1 < 0$. Then, from Theorem 2, we have that

$$p_{(1)} < p_{\gamma,b} < \frac{1-p_{\gamma,a}}{2}, \quad (157)$$

which leads to

$$p_{(1)} + p_{(2)} + p_{(3)} \leq 2p_{(1)} + p_{(3)} \quad (158)$$

$$< 2\frac{1-p_{\gamma,a}}{2} + p_{\gamma,a} \quad (159)$$

$$= 1, \quad (160)$$

where the second inequality follows since we need at least one sign change in the sequence $\{d_i\}, i \in \{1, 2, 3\}$ (see Corollary 2). Thus, we have found a contradiction since we need $p_{(1)} + p_{(2)} + p_{(3)} = 1$. This concludes the proof of Proposition 12.

C.5 Example: $p_{\min} < p_{\gamma,a}$

Let $\gamma = 0.2$ and $\mathcal{S} = \{x_1, x_2, x_3, x_4\}$ with

$$P_X(x) = \frac{1}{51} \begin{cases} 1 & x = x_1, \\ 20 & x = x_2, x_4, \\ 10 & x = x_3, \\ 0 & \text{otherwise.} \end{cases} \quad (161)$$

With this, from (18), we obtain

$$P_\gamma^* = \begin{cases} 3/154 & x = x_1, \\ 195/499 & x = x_2, x_4, \\ 191/960 & x = x_3, \\ 0 & \text{otherwise.} \end{cases} \quad (162)$$

From the above, we have that

$$d_1 = d_2 = \frac{20}{51} - \frac{195}{499} = \frac{35}{25449} > 0, \quad (163)$$

$$d_3 = \frac{10}{51} - \frac{191}{960} = -\frac{47}{16320} < 0, \quad (164)$$

$$d_4 = \frac{1}{51} - \frac{3}{154} = \frac{1}{7854} > 0, \quad (165)$$

that is, $p_{\min} = \frac{1}{51} < p_{\gamma,a}$ (see also Figure 7).

C.6 Proof of Proposition 14

We start by noting that the bounds in (36), together with the fact that $\phi(p_{(i)})$ is strictly increasing in i (see Proposition 3), implies that there is a unique k_M such that

$$k_M = \max\{i : \phi(p_{(i)}) \leq \alpha_\gamma^*\}, \quad k_M \in \mathbb{N}. \quad (166)$$

Now, we consider two cases:

1. **Case 1:** $i \leq k_M$. For this case, we have that $\phi(p_{(i)}) \leq \alpha_\gamma^*$, which implies

$$-\frac{\alpha_\gamma^*}{p_{(i)}} \leq -\frac{\phi(p_{(i)})}{p_{(i)}} = \mathbf{L}'_\gamma(p_{(i)}), \quad (167)$$

and hence, by applying $(\mathbf{L}'_\gamma)^{-1}$ on both sides of the above inequality and recalling that $(\mathbf{L}'_\gamma)^{-1}$ is strictly increasing on its domain $(-\infty, 0)$ (see Proposition 2), we arrive at

$$p_{(i)}^* \leq p_{(i)}, \quad (168)$$

that is, $d_i \geq 0$.

2. **Case 2:** $i > k_M$. For this case, we have that $\phi(p_{(i)}) > \alpha_\gamma^*$, which implies

$$-\frac{\alpha_\gamma^*}{p_{(i)}} > -\frac{\phi(p_{(i)})}{p_{(i)}} = \mathbf{L}'_\gamma(p_{(i)}), \quad (169)$$

and hence, by using similar steps as in Case 1, we arrive at

$$p_{(i)}^* > p_{(i)}, \quad (170)$$

that is, $d_i < 0$.

In summary, we have proved that $d_i \geq 0$ for all $i \leq k_M$ and $d_i < 0$ for all $i > k_M$, that is, $p_{\min} > p_{\gamma_a}$ (see also Figure 7). This concludes the proof of Proposition 14.

Remark 7. By following similar steps as above, it is not difficult to prove that, whenever $\gamma < \kappa(p_{\max})$, then $p_{\max} < p_{\gamma,b}$, that is, for these values of γ , the over-suppression regime *does* exist.

C.7 Proof of Proposition 15

We start by noting that, if $\alpha_\gamma^* < 1$, then the result trivially holds since from Corollary 2, the sequence $\{d_i\}$ has at least one sign change. Therefore, we next assume $\alpha_\gamma^* \geq 1$.

Using the definition of $\phi_\gamma(p)$ and the fact that $\phi_\gamma(p_{\gamma,b}) = \alpha_\gamma^*$, we have that

$$\alpha_\gamma^* = p_{\gamma,b} (1 - p_{\gamma,b})^{\gamma-1} \left(\gamma \log \frac{1}{p_{\gamma,b}} + \frac{1 - p_{\gamma,b}}{p_{\gamma,b}} \right) \quad (171)$$

$$\leq p_{\gamma,b} (1 - p_{\gamma,b})^{\gamma-1} \left(\frac{\gamma}{p_{\gamma,b}} - \gamma + \frac{1 - p_{\gamma,b}}{p_{\gamma,b}} \right) \quad (172)$$

$$= (1 - p_{\gamma,b})^\gamma (\gamma + 1), \quad (173)$$

where the inequality follows since $\log(x) \leq x - 1$ for $x > 0$. Now, since $\alpha_\gamma^* \geq 1$, we can further bound the above as follows,

$$1 \leq (1 - p_{\gamma,b})^\gamma (\gamma + 1), \quad (174)$$

which implies

$$p_{\gamma,b} \leq 1 - \left(\frac{1}{\gamma + 1} \right)^{\frac{1}{\gamma}}. \quad (175)$$

To show that $p_{\max} > p_{\gamma,b}$, it suffices to show that $p_{\gamma,b} < \frac{1}{|\mathcal{S}|}$ (since $p_{\max} \geq \frac{1}{|\mathcal{S}|}$). A sufficient condition for this can be obtained by setting the above upper bound to be smaller than $\frac{1}{|\mathcal{S}|}$, that is,

$$1 - \left(\frac{1}{\gamma+1}\right)^{\frac{1}{\gamma}} < \frac{1}{|\mathcal{S}|}, \quad (176)$$

or equivalently

$$\left(\frac{1}{\gamma+1}\right)^{\frac{1}{\gamma}} > \frac{|\mathcal{S}|-1}{|\mathcal{S}|}. \quad (177)$$

Since $\gamma \mapsto \left(\frac{1}{\gamma+1}\right)^{\frac{1}{\gamma}}$ is strictly increasing, it suffices to find $\gamma_0 > 0$ such that

$$\left(\frac{1}{\gamma_0+1}\right)^{\frac{1}{\gamma_0}} = \frac{|\mathcal{S}|-1}{|\mathcal{S}|} \quad (178)$$

to ensure that (177) is satisfied for all $\gamma > \gamma_0$. We now focus on solving (178), which is equivalent to

$$\left(\frac{|\mathcal{S}|}{|\mathcal{S}|-1}\right)^{\gamma_0} = \gamma_0 + 1, \quad (179)$$

or

$$\exp\left(\gamma_0 \log\left(\frac{|\mathcal{S}|}{|\mathcal{S}|-1}\right)\right) = \gamma_0 + 1. \quad (180)$$

Letting $x = \gamma_0 + 1$ (where $x > 1$) and $n = \log\left(\frac{|\mathcal{S}|}{|\mathcal{S}|-1}\right)$, we arrive at

$$\exp((x-1)n) = x, \quad (181)$$

or equivalently

$$\exp(-n) = x \exp(-nx), \quad (182)$$

or equivalently

$$-n \exp(-n) = -n x \exp(-nx). \quad (183)$$

By letting $y = -n x$ and $t = -n \exp(-n)$, we obtain

$$y \exp(y) = t. \quad (184)$$

Note that the above equation can be solved for y only if $t \geq -\frac{1}{e}$, which in our case holds since

$$t = -n \exp(-n) \quad (185)$$

$$= -\log\left(\frac{|\mathcal{S}|}{|\mathcal{S}|-1}\right) \exp\left(-\log\left(\frac{|\mathcal{S}|}{|\mathcal{S}|-1}\right)\right) \quad (186)$$

$$= \frac{|\mathcal{S}|-1}{|\mathcal{S}|} \log\left(\frac{|\mathcal{S}|-1}{|\mathcal{S}|}\right) \quad (187)$$

$$\geq \frac{1}{2} \log\left(\frac{1}{2}\right) \quad (188)$$

$$> -\frac{1}{e}, \quad (189)$$

where the inequality in (188) follows since the function in (187) is increasing in $|\mathcal{S}|$. Thus, (184) can be solved and, since $t < 0$, it has two distinct real solutions, namely

$$y = W_0(t), \quad (190)$$

and

$$y = W_{-1}(t). \quad (191)$$

We now show that the solution $y = W_0(t)$ leads to the trivial solution $\gamma_0 = 0$. We start by noting that (190) is equivalent to

$$\gamma_0 = -1 - \frac{1}{n} W_0(-n \exp(-n)). \quad (192)$$

Now, we know that $W_0(t) \in (-1, 0)$ when $-\frac{1}{e} < t < 0$ and hence, $-\frac{1}{n} W_0(t) \in (0, \frac{1}{n})$. Thus, from (192), we obtain

$$\gamma_0 = -1 - \frac{1}{n} W_0(-n \exp(-n)) \in \left(-1, -1 + \frac{1}{n}\right). \quad (193)$$

We note that $0 \in (-1, -1 + \frac{1}{n})$ and indeed $\gamma_0 = 0$ satisfies (179). However, we already know that $\gamma > 0$. Therefore, we only consider $y = W_{-1}(t)$, which is equivalent to

$$\gamma_0 = -1 - \frac{1}{n} W_{-1}(-n \exp(-n)), \quad (194)$$

where recall that $n = \log\left(\frac{|\mathcal{S}|}{|\mathcal{S}|-1}\right)$. Note also that the right-hand side of (194) is always positive. This is because $W_{-1}(t) \in (-\infty, -2 \log(2))$ when $\frac{1}{2} \log\left(\frac{1}{2}\right) \leq t < 0$ and hence, $-\frac{1}{n} W_{-1}(t) \in \left(\frac{2 \log(2)}{n}, \infty\right)$ and $\frac{2 \log(2)}{n} \geq 2$ for all $|\mathcal{S}| \geq 2$. Therefore, we conclude that $p_{\max} > p_{\gamma,b}$, whenever $\gamma > \gamma_0$. This concludes the proof of Proposition 15.

C.8 Proof of Proposition 16

We start by noting that when $p_{\min} > p_{\gamma,a}$, from Theorem 2 we have that either $p_{(i)} \in (p_{\gamma,a}, p_{\gamma,b})$ (in which case $d_i < 0$) or $p_{(i)} \in [p_{\gamma,b}, 1)$ (in which case $d_i \geq 0$) for all $i \in \{1, 2, \dots, |\mathcal{S}|\}$. Let

$$v = \min\{i : d_i < 0\}. \quad (195)$$

Then, the sequence $\{d_i\}$ has one sign change, i.e., $d_i \geq 0$ for all $i \in \{1, 2, \dots, v-1\}$ and $d_i < 0$ for all $i \in \{v, v+1, \dots, |\mathcal{S}|\}$. In addition, we also know that

$$\sum_{i=1}^{|\mathcal{S}|} d_i = 0. \quad (196)$$

A vector whose entries change sign at most once (from positive to negative) and sum to zero has all partial sums non-negative, that is, for all $k \in \{1, \dots, |\mathcal{S}|\}$, we have that

$$\sum_{i=1}^k d_i \geq 0, \quad (197)$$

or equivalently

$$\sum_{i=1}^k p_{(i)} \geq \sum_{i=1}^k p_{(i)}^*, \quad (198)$$

which, together with $\sum_{i=1}^{|\mathcal{S}|} p_{(i)} = \sum_{i=1}^{|\mathcal{S}|} p_{(i)}^* = 1$, is equivalent to $P_X \succ P_\gamma^*$. This concludes the proof of Proposition 16.

C.9 Proof of Lemma 3

To show the first property, note that for $p \in (0, 1)$, the function $\gamma \mapsto p^{(1-p)^\gamma}$ is strictly increasing and hence, $\gamma \mapsto h_\gamma(P_X)$ is strictly increasing.

To show the lower bound in the second property, note that

$$h_\gamma(P_X) \geq h_0(P_X) = \log\left(\sum_{x \in \mathcal{X}} P_X(x)\right) = 0, \quad (199)$$

where we have used the fact that $\gamma \mapsto h_\gamma(P_X)$ is strictly increasing. To prove the upper bound in the second property, we consider two cases separately:

- **Case $\gamma > 1$:** In this case, we have that

$$\sum_{x \in \mathcal{X}} P_X(x)^{(1-P_X(x))^\gamma} \quad (200)$$

$$= \sum_{x \in \mathcal{X}} e^{(1-P_X(x))^\gamma \log P_X(x)} \quad (201)$$

$$\leq \sum_{x \in \mathcal{X}} e^{(1-\gamma P_X(x)) \log P_X(x)} \quad (202)$$

$$= \sum_{x \in \mathcal{X}} P_X(x) e^{-\gamma P_X(x) \log P_X(x)} \quad (203)$$

$$\leq e^{\frac{\gamma}{e}} \sum_{x \in \mathcal{X}} P_X(x) = e^{\frac{\gamma}{e}}, \quad (204)$$

where (202) follows from the Bernoulli's inequality $(1+x)^r \geq 1+rx$, $x \geq -1, r \geq 1$; and (204) follows from the bound $x \log x \geq -\frac{1}{e}$. Thus, by using the above inside (57), we arrive at

$$h_\gamma(P_X) \leq \frac{\gamma}{e}. \quad (205)$$

- **Case $0 \leq \gamma \leq 1$:** For this case, we let

$$f(\gamma) = \sum_{x \in \mathcal{X}} P_X(x)^{(1-P_X(x))^\gamma}, \quad (206)$$

and we note that

$$f'(\gamma) = \sum_{x \in \mathcal{X}} P_X(x)^{(1-P_X(x))^\gamma} (1-P_X(x))^\gamma \log(P_X(x)) \log(1-P_X(x)) \quad (207)$$

$$\leq \sum_{x \in \mathcal{X}} P_X(x)^{(1-P_X(x))^\gamma} \log\left(\frac{1}{P_X(x)}\right) \log\left(\frac{1}{1-P_X(x)}\right) \quad (208)$$

$$\leq \sum_{x \in \mathcal{X}} P_X(x)^{(1-P_X(x))^\gamma} \quad (209)$$

$$\leq \sum_{x \in \mathcal{X}} P_X(x)^{(1-P_X(x))} \quad (210)$$

$$\leq e^{\frac{1}{e}}, \quad (211)$$

where: in (208), we have used the fact that $(1-P_X(x))^\gamma \leq 1$; (209) follows from $\log(x) \leq x-1, x > 0$; (210) is due to the fact that $\gamma \mapsto p^{(1-p)^\gamma}$ is strictly increasing; and in (211) we have used the bound in (204).

Now, by using the mean value theorem, there exists $c \in (0, \gamma)$ such that

$$f(\gamma) = f'(c)(\gamma - 0) + f(0) \quad (212)$$

$$\leq e^{\frac{1}{e}} \gamma + 1, \quad (213)$$

where in the last step we have used the bound in (211) and the fact that $f(0) = 1$.

Next, by using the above inside (57), we arrive at

$$h_\gamma(P_X) = \log(f(\gamma)) \quad (214)$$

$$\leq \log(e^{\frac{1}{e}} \gamma + 1) \quad (215)$$

$$\leq e^{\frac{1}{e}} \gamma, \quad (216)$$

where in the last step we have used the bound $\log(1+x) \leq x$.

Taking the maximum of both bounds concludes the proof of Lemma 3.

C.10 Proof of Proposition 17

To prove the first expression, we note that by using the identity in (55), we have that

$$H_\gamma(P_X, Q_X) \tag{217}$$

$$= \mathbb{E}_{X \sim P_X} \left[\log \left(\frac{1}{Q_X^{(\gamma)}(X)} \right) \right] - h_\gamma(Q_X) \tag{218}$$

$$= \mathbb{E}_{X \sim P_X} \left[\log \left(\frac{P_X(X)}{Q_X^{(\gamma)}(X)} \right) \right] - \mathbb{E}[\log P_X(X)] - h_\gamma(Q_X). \tag{219}$$

To show the second expression, we observe that

$$H_\gamma(P_X, Q_X) \tag{220}$$

$$= \sum_{x \in \mathcal{X}} P_X(x) (1 - Q_X(x))^\gamma \log \left(\frac{1}{Q_X(x)} \right) \tag{221}$$

$$= \rho_\gamma(P_X, Q_X) \left(\sum_{x \in \mathcal{X}} R_X(x) \log \left(\frac{1}{Q_X(x)} \right) \right) \tag{222}$$

$$= \rho_\gamma(P_X, Q_X) (D_{\text{KL}}(R_X \| Q_X) + H(R_X)). \tag{223}$$

This concludes the proof of Proposition 17.

C.11 Proof of Proposition 18

The lower bound follows since, from Proposition 4, we know that the mapping $\gamma \mapsto H_\gamma(P_X, Q_X)$ is non-increasing and hence,

$$\inf_{Q_X} H(P_X, Q_X) - \inf_{Q_X} H_\gamma(P_X, Q_X) \tag{224}$$

$$\geq \inf_{Q_X} H(P_X, Q_X) - \inf_{Q_X} H_0(P_X, Q_X) \tag{225}$$

$$= 0. \tag{226}$$

For the upper bound, we have that

$$\inf_{Q_X} H(P_X, Q_X) - \inf_{Q_X} H_\gamma(P_X, Q_X) \tag{227}$$

$$= \inf_{Q_X} H(P_X, Q_X) - \inf_{Q_X} \left(H(P_X, Q_X^{(\gamma)}) - h_\gamma(Q_X) \right) \tag{228}$$

$$\leq \inf_{Q_X} H(P_X, Q_X) - \inf_{Q_X} H(P_X, Q_X^{(\gamma)}) + \sup_{Q_X} h_\gamma(Q_X) \tag{229}$$

$$\leq \inf_{Q_X} H(P_X, Q_X) - \inf_{Q_X} H(P_X, Q_X) + \sup_{Q_X} h_\gamma(Q_X) \tag{230}$$

$$= \sup_{Q_X} h_\gamma(Q_X) \tag{231}$$

$$\leq e^{\frac{1}{e}} \gamma, \tag{232}$$

where: (228) follows from (59); (229) is due to the fact that $\inf_x (f(x) - g(x)) \geq \inf_x f(x) - \sup_x g(x)$, which follows since $f(x) \geq \inf_x f(x)$ and $g(x) \leq \sup_x g(x)$; (230) is due to the fact that the space over which $Q_X^{(\gamma)}$ is defined is a subset of $\mathcal{P}(\mathcal{X})$; and in (232) we have used the bound in Lemma 3. This concludes the proof of Proposition 18.

D Experiments on Synthetic Data

We consider two classes $C \in \{0, 1\}$ with $P[C = 0] = 0.95$ and $P[C = 1] = 0.05$, and two features $F_1 \in \{0, 1, 2, 3\}$ and $F_2 \in \{0, 1, 2, 3\}$. Note that this is an example of an imbalanced dataset. We let

$$P[F_1 | C = 0] = [0.65, 0.20, 0.10, 0.05], \tag{233}$$

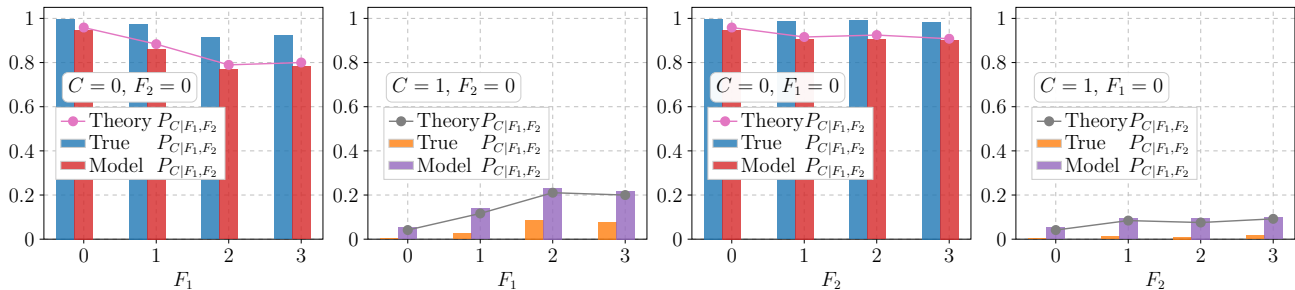


Figure 12: Synthetic dataset. For each class, we fixed one of the features at its modal value and plot: the true posterior, the posterior predicted by the trained neural network, and the theoretical focal-entropy minimizer.

$$P[F_1|C=1] = [0.10, 0.25, 0.45, 0.20], \quad (234)$$

$$P[F_2|C=0] = [0.50, 0.30, 0.15, 0.05], \quad (235)$$

$$P[F_2|C=1] = [0.20, 0.50, 0.20, 0.10]. \quad (236)$$

We assume that the two features are conditionally independent given the class, i.e., $P[F_1, F_2|C] = P[F_1|C]P[F_2|C]$. From this, we can therefore obtain the joint probability mass function as follows,

$$P[F_1, F_2, C] = P[F_1|C]P[F_2|C]P[C], \quad (237)$$

and, by the Bayes' rule, also get $P[C|F_1, F_2]$ (see the bars labeled as “True $P_{C|F_1, F_2}$ ” in Figure 12 for some examples). We used this $P_{C|F_1, F_2}$ inside (18) to obtain P_γ^* for $\gamma = 1$, i.e., $P_\gamma^* = \arg \min_{Q_X} H_\gamma(P_{C|F_1, F_2}, Q_X)$ (see the bars labeled as “Theory $P_{C|F_1, F_2}$ ” in Figure 12 for some examples).

We generated 10,000 samples by repeatedly sampling from the 16 possible two-dimension feature vector space (i.e., two features with four possible values each, and two classes). These samples were used to train a feedforward neural network with a single hidden layer of 64 neurons, each using the ReLU activation function. We trained this model by using the focal loss in (3) with $\gamma = 1$ and performed the optimization with the Adam optimizer at a learning rate of 10^{-3} . Training was carried out with a batch size of 64 over 30 epochs. The trained neural network produced predicted probabilities for each of the two classes by applying the softmax function to the output layer (see the bars labeled as “Model $P_{C|F_1, F_2}$ ” in Figure 12 for some examples). From Figure 12, we observe that the neural network output probability is close to P_γ^* in (18) (i.e., with a maximum difference of 0.027). This not only supports our theoretical analysis, but it also shows that the neural network has effectively converged to the global minimum, achieving the best possible performance under the focal loss.

References

- M. M. Al Rahhal, Y. Bazi, H. Almubarak, N. Alajlan, and M. Al Zuair. Dense convolutional networks with focal loss and image generation for electrocardiogram classification. *IEEE Access*, 7:182225–182237, 2019.
- Han Bao and Nontawat Charoenphakdee. Calm composite losses: Being improper yet proper composite. In *The 28th International Conference on Artificial Intelligence and Statistics*, 2025.
- Jonas R Brehmer and Tilmann Gneiting. Properization: Constructing proper scoring rules via Bayes acts. *Annals of the Institute of Statistical Mathematics*, 72(3):659–673, 2020.
- A. Buja, W. Stuetzle, and Y. Shen. Loss functions for binary class probability estimation and classification: Structure and applications. *Working draft, November*, 3:13, 2005.
- K. Cao, C. Wei, A. Gaidon, N. Arechiga, and T. Ma. Learning imbalanced datasets with label-distribution-aware margin loss. In *Adv. Neural Inf. Process. Syst. (NeurIPS)*, volume 32, pages 1565–1576, 2019.
- N. Charoenphakdee, J. Vongkulbhisal, N. Chairatanakul, and M. Sugiyama. On focal loss for class-posterior probability estimation: A theoretical perspective. In *Proc. IEEE/CVF Conf. Computer Vision and Pattern Recognition (CVPR)*, pages 5202–5211, 2021.
- R. M. Corless, G. H. Gonnet, D. E. G. Hare, D. J. Jeffrey, and D. E. Knuth. On the lambert w function. *Advances in Computational Mathematics*, 5(1):329–359, 1996.

- T. M. Cover and J. A. Thomas. *Elements of Information Theory (2nd edn)*. Wiley, 2006.
- Y. Cui, M. Jia, T.-Y. Lin, Y. Song, and S. Belongie. Class-balanced loss based on effective number of samples. In *Proc. IEEE/CVF Conf. Computer Vision and Pattern Recognition (CVPR)*, pages 9268–9277, 2019.
- J. Dougherty, R. Kohavi, and M. Sahami. Supervised and unsupervised discretization of continuous features. In *Machine Learning Proc. 1995*, pages 194–202. Elsevier, 1995.
- A. Dytso and M. Cardone. Lossy source coding with focal loss. *arXiv preprint arXiv:2504.19913*, 2025.
- G. B. Folland. *Real Analysis: Modern Techniques and Their Applications*. Wiley, New York, 2 edition, 1999.
- A. Ghosh, T. Schaaf, and M. Gormley. Adafocal: Calibration-aware adaptive focal loss. *Adv. Neural Inf. Process. Syst. (NeurIPS)*, 35:1583–1595, 2022.
- H. He and E. A. Garcia. Learning from imbalanced data. *IEEE Transactions on Knowledge and Data Engineering*, 21(9):1263–1284, 2009.
- D. Impedovo and G. Pirlo. Zoning methods for handwritten character recognition: A survey. *Pattern Recognit.*, 47(3):969–981, 2014.
- M. Jeong, M. Cardone, and A. Dytso. Demystifying the optimal performance of multi-class classification. In *Thirty-seventh Conference on Neural Information Processing Systems*, 2023. URL <https://openreview.net/forum?id=p9k5MS0JAL>.
- T. O. Kväseth. Entropies and their concavity and schur-concavity conditions. *IEEE Access*, 10:96006–96015, 2022.
- Z. Leng, M. Tan, C. Liu, E. D. Cubuk, X. Shi, S. Cheng, and D. Anguelov. Polyloss: A polynomial expansion perspective of classification loss functions. *arXiv preprint arXiv:2204.12511*, 2022.
- X. Li, X. Sun, Y. Meng, J. Liang, F. Wu, and J. Li. Dice loss for data-imbalanced nlp tasks. In *Proceedings of the 58th Annual Meeting of the Association for Computational Linguistics*, pages 4658–4669, 2020a.
- X. Li, W. Wang, L. Wu, S. Chen, X. Hu, J. Li, J. Tang, and J. Yang. Generalized focal loss: Learning qualified and distributed bounding boxes for dense object detection. *Adv. Neural Inf. Process. Syst. (NeurIPS)*, 33: 21002–21012, 2020b.
- X. Li, C. Lv, W. Wang, G. Li, L. Yang, and J. Yang. Generalized focal loss: Towards efficient representation learning for dense object detection. *IEEE Trans. Pattern Anal. Mach. Intell.*, 45(3):3139–3153, 2022.
- J. Lin, X. Jin, and C. Zhang. Tce: Tilted cross-entropy loss for classification. In *Proc. IEEE/CVF Conf. Computer Vision and Pattern Recognition Workshops (CVPRW)*, pages 4061–4070, 2021.
- T.-Y. Lin, P. Goyal, R. Girshick, K. He, and P. Dollár. Focal loss for dense object detection. In *Proc. IEEE Int. Conf. Computer Vision (ICCV)*, pages 2980–2988, 2017.
- J. Mukhoti, V. Kulharia, A. Sanyal, S. Golodetz, P. H. S. Torr, and P. Dokania. Calibrating deep neural networks using focal loss. *Advances in Neural Information Processing Systems (NeurIPS)*, 33:15288–15299, 2020.
- B. Peters, V. Niculae, and A. F. T. Martins. Sparse sequence-to-sequence models. In *Proc. 57th Annu. Meeting Assoc. Computational Linguistics (ACL)*, pages 1504–1519, 2019.
- M. Ren, W. Yu, J. Ma, S. Zhao, H. Li, and R. Urtasun. Balanced meta-softmax for long-tailed visual recognition. In *Adv. Neural Inf. Process. Syst. (NeurIPS)*, volume 33, pages 4175–4186, 2020.
- W. Shu, S. Wang, Q. Chen, Y. Hu, Z. Cai, and R. Lin. Pathological image classification of breast cancer based on residual network and focal loss. In *Proceedings of the 2019 3rd International Conference on Computer Science and Artificial Intelligence*, pages 211–214, 2019.
- J. Vongkulbhisal, P. Vinayavekhin, and M. Visentini-Scarzanella. Unifying heterogeneous classifiers with distillation. In *Proceedings of the IEEE/CVF Conference on Computer Vision and Pattern Recognition*, pages 3175–3184, 2019.
- Y. Zhang, C. Chen, H. Shi, M. Song, Y. Wu, and J. Zhang. Dual focal loss for calibrated classification. In *Proc. 40th Int. Conf. Machine Learning (ICML)*, 2023.